Published in final edited form as:
Health Phys. 2012 March ; 102(3): 305–325.

Guidance on the Use of Hand-Held Survey Meters for Radiological Triage: Time-Dependent Detector Count Rates Corresponding to 50, 250, and 500 mSv Effective Dose for Adult Males and Adult Females

Wesley E. Bolch, PhD,
Departments of Nuclear & Radiological and Biomedical Engineering, University of Florida, Gainesville, FL 32611

Jorge L. Hurtado, MS,
Department of Nuclear & Radiological Engineering, University of Florida, Gainesville, FL 32611

Choonsik Lee, PhD,
Division of Cancer Epidemiology and Genetics, National Cancer Institute, National Institutes of Health, Bethesda, Maryland 20852

Ryan Manger, MS,
Department of Mechanical Engineering, Georgia Institute of Technology, Atlanta, GA

Nolan Hertel, PhD, and
Department of Mechanical Engineering, Georgia Institute of Technology, Atlanta, GA

William Dickerson, MD
Consultant, Bethesda, MD

Abstract

In June of 2006, the Radiation Studies Branch of the Centers for Disease Control and Prevention held a workshop to explore rapid methods of facilitating radiological triage of large numbers of potentially contaminated individuals following detonation of a radiological dispersal device. Two options were discussed. The first was the use of traditional gamma-cameras in nuclear medicine departments operated as make-shift whole-body counters. Guidance on this approach is currently available from the CDC. This approach is feasible if a manageable number of individuals were involved, transportation to the relevant hospitals was quickly provided, and the medical staff at each facility had been previously trained in this non-traditional use of their radiopharmaceutical imaging devices. If, however, substantially large numbers of individuals (100s to 1000s) needed radiological screening, other options must be given to first responders, first receivers, and health physicists providing medical management. In this study, the second option of the workshop was investigated – the use of commercially available portable survey meters (either NaI or GM based) for assessing potential ranges of effective dose (<50, 50–250, 250–500, and >500 mSv). Two hybrid computational phantoms were used to model an adult male and an adult female subject internally contaminated with either ^{241}Am, ^{60}Cs, ^{137}Cs, ^{131}I, and ^{192}Ir following an acute inhalation or ingestion intake. As a function of time following the exposure, the net count rates corresponding to committed effective doses of 50, 250, and 500 mSv were estimated via Monte Carlo radiation transport simulation for each of four different detectors types, positions, and

For reprints and correspondence contact: Wesley E. Bolch, PhD, PE, CHP Director, Advanced Laboratory for Radiation Dosimetry Studies (ALRADS) Department of Nuclear and Radiological Engineering University of Florida, Gainesville, Florida 32611-8300 Phone: (352) 846-1361 Fax: (352) 392-3380 wbolch@ufl.edu.

screening distances. Measured count rates can be compared to these values and an assignment of one of four possible effective dose ranges could be made. The method implicitly assumes that all external contamination has been removed prior to screening, and that the measurements be conducted in a low-background, and possibly mobile, facility positioned at the triage location. Net count rate data are provided in both tabular and graphical format within a series of eight handbooks available at the CDC website http://emergency.cdc.gov/radiation.

Keywords

Radiological triage; first responders; radiological dispersion device; radiation survey meter

INTRODUCTION

Events in which individuals may become internally contaminated with radionuclides can span a wide range of possible scenarios. At one extreme, the event may be an accidental exposure in a medical, industrial, or research setting involving only a few persons. Dose assessments to these individuals may involve bioassay analysis or potentially whole-body counting, following by medical decisions based on projected organ and/or effective dose. These types of situations are discussed in detail within Report No. 65 on *Management of Persons Accidentally Contaminated with Radionuclides*, by the National Council on Radiation Protection and Measurement (NCRP 1980), and in its forthcoming revision by NCRP Scientific Committee 4-1 (www.ncrponline.org). At the other extreme, a radiological terrorist event may involve dispersal of a radionuclide through conventional explosives (i.e., radiological dispersal device or RDD) (NCRP 2001), with some tens to perhaps a few tens of individuals potentially contaminated. In this case, other means of dose assessment and medical triage decision would be needed. The Radiation Studies Branch of the Centers for Disease Control and Prevention (CDC) has posted guidance on the use of nuclear medicine gamma-cameras as make-shift whole-body counters to handle these types of larger events, with the argument that access to and availability of equipment within nuclear medicine departments will be preferable to transporting potentially unmanageable numbers of individuals to specialized nuclear facilities with whole-body counters. Reports on this method can be found on the CDC Radiation Studies Branch homepage (see http://emergency.cdc.gov/radiation).

If, however, hundreds to thousands of individuals are potentially contaminated following an RDD detonation, or possibly a small nuclear weapons terrorist attack, more rapid radiological triage methods should be in place so as to properly assignment hospital and medical resources accordingly. In its revision to Report No. 65, the NCRP presents a nine-stage response plan for dealing with persons contaminated with radionuclides (see Fig. 1). Following medical and external decontamination assessment in areas near the event (Stages 1 to 3), those with the potential for internal radionuclide deposition are transported to a regional hospital or other medical facility where medical evaluations (Stage 4), internal dose assessments (Stage 5), clinical decisions (Stage 6), and potential therapy interventions (Stage 7) would be made.

In June of 2006, the CDC Radiation Studies Branch hosted a workshop to discuss potential research into the use of portable survey meters for conducting radiological triage screening of individuals near hospital facilities. These evaluations would be conducted under NCRP Stage 4 evaluations in a shielded (i.e., low background) semi-trailer or other portable facility through which individuals would be sent following Stage 3 external decontamination. Survey meter measurements would be taken, with the resulting net count rates used to estimate the range of potential effective dose to each exposed individual. Decisions could

then be made regarding estimated ranges of effective dose based on interpretation of the measured values against those determined by biokinetic modeling and Monte Carlo phantom simulations of detector response using reference phantoms. The use of survey meters would be a first approximation in sorting individuals into ranges of effective dose. If residual external contamination were still present (e.g., activity tenaciously retained in hair), this contribution would have to estimated in some fashion in the adjustment of the net count rate; otherwise, the estimated range of effective dose would be conservatively assigned. Final decisions on medical therapy for those in higher dose categories would need to await verification under Stage 5 excreta bioassay or whole-body counting techniques.

The present study was initiated in response to this CDC workshop. Our objectives were (1) to develop a pair of hybrid computational phantoms representing the ICRP reference adults – both male and female (yet scalable to non-reference height and age percentile distributions), and (2) use these phantoms to simulate individuals with inhaled or ingested radioactivity following the detonation of a radiological dispersion device. These hybrid phantoms, described in detail in Hurtado *et al*. (this issue), were used to assess the photon energy fluence at both the anterior and posterior surfaces for five different radionuclides of interest, and all relevant source tissues. These photon fluence maps were then used to determine detector count rate efficiencies in one GM-based and three NaI-based survey meters at various anatomical positions and measurement distances. Time-dependent detector net count rate were thus established corresponding to 50, 250, and 500 mSv of effective dose. Measured net count rates would then be used to sort individuals within one of four dose categories: < 50 mSv, between 50 and 250 mSv, between 250 and 500 mSv, and greater than 500 mSv. Guidance on the use of hand-held survey meters for rapid radiological triage as outlined in this study are provided in handbook form at http://emergency.cdc.gov/radiation.

MATERIALS AND METHODS

Hybrid phantoms representing internally contaminated adults

In this study, two hybrid computational phantoms were used to represent an adult male and an adult female both internally contaminated with radioactivity following an acute inhalation or ingestion exposure. Details of their construction are given in Hurtado *et al*.(this issue). As described, the reference voxel phantoms were created at isotropic voxel resolutions of (1.58 mm)^3 for the male phantom and (1.26 mm)^3 for the female phantom. In this study, however, voxel phantoms of a slightly coarser resolution of 2 mm × 2 mm × 2 mm were created for computational efficiency in the Monte Carlo simulations of detector response.

Exposure scenarios

A total of 21 exposure scenarios were considered in this study covering five radionuclides of potential use in a radiological dispersion device. These radionuclides are^{241}Am, ^{60}Co, ^{137}Cs, ^{131}I, and ^{192}Ir as listed in Table 1. For each radionuclide, one ingestion exposure scenario was considered, along with various inhalation exposure scenarios for different combinations of particle size distribution (1 or 5 μm AMAD) and lung solubility class (Type F, M, or S) as defined in the ICRP Publication 66 Human Respiratory Tract Model (HRTM) (ICRP 1994). For inhalation exposures, only those combinations of particle size and lung solubility were considered for which dose coefficients (Sv per Bq-intake) are provided in ICRP Publication 72 (ICRP 1996) and ICRP CD No. 1 (ICRP 2002). Consequently, as shown in Table 1, only two inhalation exposure scenarios were considered for ^{241}Am (1 μm and 5 μm AMAD) with dose coefficients provided for only Type M materials. Conversely, variations and uncertainties in both particle size and

lung solubility for compounds incorporating ^{192}Ir require the assessment of all six combinations of inhalation exposure (2 particle sizes and 3 solubility classes).

Further information on RDD aerosol and material characteristics of RDD can be found in Harper et al. (2007). Table 3 of that study indicates that if an RDD device is constructed using either ^{60}Co or ^{192}Ir, then metallic aerosol fragments will most likely be produced. Consequently, our Type F scenario for ^{192}Ir will thus be highly unlikely. They are given, however, for completeness and consistency with tabulations of ICRP dose coefficients.

Table 1 additionally summaries the effective dose per unit activity intake (Sv per Bq-intake) for all 21 scenarios. Effective dose coefficients for the three ^{241}Am exposure scenarios are significantly higher (~ 10^{-7} Sv Bq^{-1} for ingestion and ~10^{-5} Sv Bq^{-1} for inhalation) than found for the other four radionuclides (~10^{-8} to 10^{-9} Sv Bq^{-1}). Consequently, it will be seen that the detector count rates required to realize a given triage value of effective dose will be significantly lower for ^{241}Am than the other four radionuclides by these same orders of magnitude – assuming no change in detector, location, and screening distance. Table 1 additionally provides values of the equivalent dose coefficient for lungs, red bone marrow, and thyroid for a 30-day dose integration period. While this study focuses on assessing ranges of effective dose using portable survey meter measurements near contaminated individuals, triage decisions may additionally be based on estimated equivalent doses to critical organs, although the likelihood for reaching deterministic threshold doses following acute inhalation exposure is exceedingly small.

Biokinetic modeling

An important parameter for predicting survey meter response is the fractional amount of the radionuclide intake present in a given source organ of the contaminated individual as a function of time post-intake. These values of f_S (t) (Bq in source organ S per unit Bq intake) were taken in this study from the DCAL software provided by the Center for Biokinetic and Dosimetry Research at the Oak Ridge National Laboratory (ordose.ornl.gov). The cumulative activity retained within the total body f_{TB} (t) is then defined such that f_{TB}

$$f_{TB}(t)=\sum_{S} f_s(t)$$

Derivation of detector response functions and count rate thresholds

The committed effective dose E (in Sv) to a radioactively contaminated individual can be estimated as the product of the radionuclide intake I (in Bq) and an ICRP effective dose coefficient e(in Sv / Bq). The estimate of the radionuclide intake Ican in turn be estimated as the ratio of the total body activity A_{TB} (t) at time t post-intake and the fractional total body retention of the radionuclide f_{TB} (t) *also* assessed at time t post-intake (taken from the DCAL program). The resulting expression is given as:

$$E(Sv)=\left[I(Bq_{intake})\right]\left[e\left(\frac{Sv}{Bq_{intake}}\right)\right]=\frac{\left[A_{TB}(t)(Bq_{TB})\right]\left[e\left(\frac{Sv}{Bq_{intake}}\right)\right]}{\left[f_{TB}(t)\left(\frac{Bq_{TB}}{Bq_{intake}}\right)\right]} \quad (1)$$

For a detector at position x near the body of the potentially contaminated person (front of the chest wall at 30 cm distance, for example), an estimate of total body activity at time t post-intake can be estimated as:

$$A_{TB}^{x}(t)(Bq_{TB})=\frac{\left[r_{D}^{x}(t)(cps)\right]}{\left[\varepsilon_{D}^{x}(t)\left(\frac{cps}{\gamma_{TB}/s}\right)\right]\left[Y_{total}\left(\frac{\gamma_{TB}/s}{Bq_{TB}}\right)\right]} \quad (2)$$

where $r_{D}^{x}(t)(t)$ is the detector net count rate (counts per second – cps) assessed at position x at time *t* post-intake, $\varepsilon_{D}^{x}(t)(t)$*is* the absolute detector efficiency (counts registered per emitted photon emitted from within the total body) which is also time and position dependent, and Y_{total} is the total yield of x-ray and gamma-ray photons emitted by the radionuclide (photons per second per Bq in the total body). As each detector can potentially receive uncollided as well as scattered photons generated from multiple source organs in the body (which differ as a function of time post-intake), the time-dependent absolute detector efficiency at position x can be estimated as:

$$\varepsilon_{D}^{x}(t)\left(\frac{cps}{\gamma_{TB}/s}\right)=\sum_{S}\left[\varepsilon_{MC,S}^{x}\left(\frac{c}{\gamma_{S}}\right)\right]\left[f_{S}^{Norm}(t)\left(\frac{\gamma_{S}}{\gamma_{TB}}\right)\right] \quad (3)$$

where $\varepsilon_{MC,S}^{x}$ is the number of registered detector counts at position x per simulated photon emitted from source organ *S* (determined via Monte Carlo radiation transport within the computational phantom and for that radionuclide of interest), and $f_{S}^{Norm}(t)(t)$ is the normalized fraction of total body activity in source organ *S* at time *t* post-intake. As given in Eqn. 3, the detector absolute efficiency for the radionuclide at time *t* post-intake is thus a weighted average of its values for individual source organs within the phantom (a value which is time independent and need be assessed only once for a given phantom, source organ, and detector type and position). Finally, the total yield of the emitted photons per unit activity of the radionuclide is simply the summation of the energy-dependent photon yields across the energy spectrum of x-rays and gamma-rays for that radionuclide:

$$Y_{total}\left(\frac{\gamma_{TB}/s}{Bq_{TB}}\right)=\sum_{i}Y_{i}\left(\frac{\gamma_{i}}{transformation}\right) \quad (4)$$

where Y_i is the number of photons of energy *i* per decay of the radionuclide. As used in Eqn. 2, Eqn. 4 has implicit units of photons emitted per second *in the total body* per Bq activity *in the total body*. In this study, we utilize the photon spectrum for each radionuclide as given in Eckerman and Endo (2008).

Using Eqns. 2 to 4, Eqn. 1 may be rewritten to give a final expression for the estimating the contaminated person's committed effective dose given an acute inhalation or ingestion:

$$E(Sv)=\frac{\left[r_{D}^{x}(t)(cps)\right]\left[e\left(\frac{Sv}{Bq_{intake}}\right)\right]}{\left\{\sum_{S}\left[\varepsilon_{MC,S}^{x}\left(\frac{c}{\gamma_{S}}\right)\right]\left[f_{s}^{Norm}(t)\left(\frac{\gamma_{S}}{\gamma_{TB}}\right)\right]\right\}\left[\sum_{i}Y_{i}\left(\frac{\gamma_{TB}}{Bq_{TB}}\right)\right]\left[f_{TB}(t)\left(\frac{Bq_{TB}}{Bq_{intake}}\right)\right]} \quad (5)$$

By collapsing terms, Eqn. 5 can alternatively be expressed as the product of a net detector count rate (either cps or cpm) and a time-dependent effective dose response function$R_{E}^{x}(t)$:

$$E(Sv)=\left[r_{D}^{x}(t)(cps)\right]\left[\mathbf{R}_{E}^{x}(t)\left(\frac{Sv}{cps}\right)\right]\text{or}E(mSv)=\left[r_{D}^{x}(t)(cpm)\right]\left[\mathbf{R}_{E}^{x}(t)\left(\frac{mSv}{cpm}\right)\right]. \quad (6)$$

Finally, time-dependent net count rate thresholds r^{x}_{Thres} (in cpm) corresponding to a given effective dose threshold (50, 250, or 500 mSv) which can trigger a certain set of radiological triage decisions may be estimated as follows:

$$r^{x}_{Thres}(t)(cpm) = \frac{E_{Thres}(mSv)}{\mathbf{R}^{x}_{E}\left(\frac{mSv}{cpm}\right)}, \quad (7)$$

where E_{Thres} is set to either 50 mSv, 250 mSv, and 500 mSv, respectively, in this study. As described later, individuals may then be sorted into one of four dose categories: (1) below 50 mSv, (2) between 50 and 250 mSv, (3) between 250 and 500 mSv, and (4) exceeding 500 mSv. Medical decisions may then be made under Stages 5, 6, and 7 depending on the dose category assigned. While the method presented here is for rapid sorting of large numbers of individuals, higher dose categories should be verified under Stage 4 using more sophisticated techniques (e.g., bioassay or whole-body counting) given available time and resources before proceeding to these other stages.

Phantom source regions and surface photon fluences

Table 2 summaries the various source regions modeled for each of the five radionuclides considered in the study. Check marks indicate those source organs for which explicit values of $\varepsilon^{x}_{MC,S}$ were assessed via radiation transport simulation. Organs indicated by dots in Table 2 are those which never exceed 1% of the intake activity, and in this study, their estimated fractional activity was folded into the larger source region called *Other Tissues*. This category was modeled in the computational phantoms as the collection of all soft tissues for which an explicit value of $f_S(t)$ was not already specified as indicted in Table 2. For blood sources, Table 2.14 of ICRP Publication 89 was consulted. As many of the tissues in this table have reference values less than 1% of total blood volume, a collapsed table of percentages was implemented in the study as shown on the right side of Table 3. Total blood volume was thus modeled using 12 source regions, with their percent distribution being the same for the adult male and female.

For each of the 100 combinations of radionuclide, phantom gender, and source organ as given in Table 2, a total of 10^7 photon histories were simulated using the MCNPX radiation transport code. The full photon spectra were sampled for each simulation using the energies and yields given in the data tables of Eckerman and Endo (2008) for each of the 5 radionuclides. For each simulation, the energies and emission angles of all photons exiting the phantoms were recorded on one of two different rectangular surfaces – one at the front and one at the back of the phantom tangential to the body surface. By using these surface-source writes (or SSW in the terminology of the MCNPX code), subsequent radiation transport to the various detector models (see below) could be accomplished with high computational efficiently and without the need for re-modeling photon transport internally within either phantom.

MCNPX detector models

Four different geometrical models of various survey-type radiation detectors were constructed for input to the MCNPX radiation transport code. These detectors are (A) the NaI-based Ludlum 375-30 waste monitor, (B) the NaI-based Ludlum 44-17 low-energy gamma scintillator probe, (C) the NaI-based Ludlum 12S survey meter, and (D) the Ludlum 44-9 pancake GM probe. Detectable pulses within the sensitive volume of each detector were registered (via the F8 pulse-height tally) for each energy deposition event exceeding 30 keV (e.g., lower-level discriminator) for the NaI scintillator systems, and 10 keV for the GM detector. Transport of secondary electrons was performed for simulations involving the

pancake GM probe, while the kerma approximate (i.e., no secondary electron transport) was applied for the three NaI-based detectors. Test runs were performed with and without secondary electron transport for the NaI-based detectors, with resulting pulse height tallies differing no more than 1–2%.

For each exposure scenario, four copies of the detector models were created within MCNPX corresponding to four different anatomical locations as demonstrated in Figure 2 for the adult male phantom. Applying the descriptors anterior (A) and posterior (P), these positions are denoted as*AP chest* (center of the sternum in the front of the phantom) and*AP abdomen* (aligned with the navel in the front of the phantom), along with the corresponding *PA chest* and *PA abdomen*positions at the back of the phantom. Furthermore, four different distances from the phantom surface were also considered: 6 cm, 30 cm, 100 cm, and 200 cm. For each detector type and distance, each of the 100 MCNPX surface source writes were used to model the transport of photons emerging from both the front and back surfaces of the phantom through the surrounding air space, with a fraction of these incident upon one of the four different detectors positions, all located at the same surface-to-detector distance. A total of four sequential Monte Carlo simulations were then made were (one at each distance) for each phantom (male or female), each source organ, and each radionuclide. For each simulation, however, four values of $\varepsilon^{x}_{MC,S}$ were recorded simultaneously - one for each of the four detector positions (AP chest, AP abdomen, PA chest, or PA abdomen). A brief description of each detector model is given below.

Statistical errors on values of $\varepsilon^{x}_{MC,S}$ varied significantly among the various source organs for a given detector position, with the highest uncertainties given for ET_1 sources contributing to detector counts in the PA abdomen position. On average, statistical errors on detector absolution efficiencies were ~1–2% at distances of 6 and 30 cm, were ~5% at 100 cm, and were ~10% at a screening distance of 200 cm. These statistical errors were considered acceptable given much larger uncertainties in individual subject biokinetics and body morphometry.

Ludlum 375-30 Waste Monitor—The MCNPX geometric model for this detector is shown in Figure 3A and was based on schematic diagrams provided to us from Ludlum Measurements, Inc. This detector was chosen as a representative that used for portal monitoring in a hospital setting and was previously used in CDC funded studies at the Hershey Medical Center (see http://www.bt.cdc.gov/radiation/). The detector sensitive volume is a 3 inch × 1 inch NaI crystal enclosed in a lead collimator casing.

Ludlum 44-17 Low-Energy Gamma Scintillator—Several options were considered for the selection of an appropriate thyroid probe for simulation including the availability of engineering schematics and material composition data. The model chosen, due to cooperation by the manufacturer, was the Ludlum 44-17 low-energy gamma scintillator as shown in Figure 3B. Monthly thyroid bioassays are performed at the University of Florida using this detector model along with various output devices. For the present study, only the probe itself was considered during radiation transport simulations. The Ludlum 44-17 probe contains a 2 inch × 2 mm thick NaI crystal encased in an aluminum cylinder with a Mylar cover for protection against dust and foreign particles. The Model 44-17 also contains very little shielding between the crystal and the individual being screened.

Ludlum 12S Survey Meter—The MCNPX geometric model for this detector is shown in Figure 3C, and was selected as representative of a portable handheld survey meter of potential use by first responders following an RDD event. A computational model for this detector was constructed using both (1) physical measurements of the actual device, and (2)

schematic diagrams provided by the manufacturer. Items physically measured included the exterior wall thickness, battery compartment depth, and circuit board thicknesses. Any measurements inaccessible to physical measurement were requested from Ludlum Measurements, Inc, along with information on material composition and density. The Model 12S detector contains a 1 inch × 1 inch NaI crystal inside an aluminum housing. The housing is situated within an aluminum detector casing which also incorporates the battery case and two circuit boards. The remainder of the detector was considered air-filled at standard pressure and temperature.

Ludlum 44-9 GM Probe—Figure 3D displays our MCNPX detector model for the Ludlum 44-9 pancake GM probe. This probe was modeled based upon combinations of physical measurement and manufacturer-provided schematics. The wire mesh covering and Mica window were modeled, along with the probe handle. Detailed information was not available (from the contractor used by Ludlum for this specific probe) regarding either the pressure of the fill gas or the identify of the quench gas. Consequently, approximate values were assumed (100% neon fill gas at one atmosphere). Next, correction factors for the GM probe MCNP tally results were obtained via a combination of experimental measurement and MCNP modeling of those same experiments. A slab phantom as shown in Figure 4 was used consisting of 100 mm of Virtual Water as a backscatter medium, a Lucite source holder, and various additional layers of Lucite attenuators. Ludlum 44-9 GM probe counts rates were recorded at distances of 0, 6, and 12 mm from the source slab enclosing radioactive check sources of either ^{241}Am, ^{133}Ba, ^{137}Cs, ^{60}Co, ^{54}Mn, or ^{22}Na. The detector was placed on the surface of the outer layer of the Lucite slab phantom to ensure consistency. Additionally, the slab phantom, Lucite attenuators, and detector probe (same as that used in the human phantom simulations) was additionally modeled in MCNP and a pulse height tally (F8) was performed over the gas volume within the GM tube. Ratios of count rates acquired via MCNP simulation to those experimentally measured were then assembled for each radionuclide, and the results averaged to form an MCNP correction factor to account for uncertainties in fill gas composition and density. These corrections factors were subsequently used in the determination of the count rate thresholds via Eqns. 5–7.

RESULTS

Detector handbook series at the CDC Radiation Studies Branch website

Photon spectral data, MCNPX detector efficiencies, and DCAL values of time-dependent fractional organ burdens were evaluated according to Eqns. 5 to 7 in the assembly of a large database of count rate thresholds corresponding to 50, 250, and 500 mSv effective dose. Values are given in the data base for both the adult male and adult female subject across all 21 exposure scenarios, four detector designs, four screening distances, and four anatomical screening positions. The data are organized as a series of eight handbooks accessible via the CDC Radiation Studies Branch website http://emergency.cdc.gov/radiation. Each handbook corresponds to one detector type and one screening subject (either the adult male or adult female) as outlined in Table 4. Each handbook includes an index to the 21 exposure scenario tables along with instructions for handbook use and radiological triage decisions.

Table 5 displays representative data from Table F6 of Handbook F for radiological triage screening of the reference adult female at distances of 6 cm (upper table highlighted in tan) or at 30 cm (lower table highlighted in rose) from the body surface. Table 6 displays corresponding data for triage screening at 100 cm (color-coded yellow) and at 200 cm (color-coded blue) from the body surfaces. These tables correspond to an acute inhalation of a 5-μm AMAD ^{60}Co aerosol of Type M lung solubility (Exposure Scenario 6 as per Table

1). As a function of time extending out to 30 days post-intake, net count rates for the Ludlum 12s survey meter are estimated for four different detector positions (AP chest, AP abdomen, PA chest, or PA abdomen) and three effective dose levels (50, 250, and 500 mSv). At a screening distance of 200 cm, the photon fluence differs minimally between chest and abdominal detector positions (being relatively far from the subject), and thus only a single average estimate count rate threshold is given at that distance.

These same data are additionally given in graphical form in the Handbooks as shown in both Figure 5 (left side – 6 cm and right side – 30 cm) and in Figure 6 (left side – 100 cm and right side – 200 cm). Upper plots within Figures 5 and 6 correspond to measurements made while the subject is facing toward the screener, while lower plots correspond to measurements made with the subject facing away from the screener. In each case, dose levels are indicated by color with blue, green, and red curves corresponding to 50, 250, and 500 mSv effective dose, respectively. Furthermore, solid curves of a given color correspond to chest-level measurements (AP chest – upper plots and PA chest – lower plots), while dashed curves of a given color correspond to abdominal-level measurements (AP abdomen – upper plots and PA abdomen – lower plots). The time axis is given on a logarithmic scale where the first decade (0.01 to 0.1 days) corresponds to times of between ~15 minutes to ~2.5 hours, the second decade (0.1 to 1 day) corresponds to times of between ~2.5 hours and 1 day, and remainder of the abscissa extends to 30 days post-exposure (1 month).

According to the engineering staff at Ludlum Measurements, Inc.,[1] the maximum count rate prior to significant detector saturation and/or loss of linear response is approximately 875,000 cpm for the three Ludlum NaI-based detectors of this study, and is approximately 100,000 cpm for the GM pancake probe. Consequently, the handbooks are designed to instruct the user to avoid combinations of exposure time, screening position, and screening distance that would – accordingly to the reference anatomical and biokinetic models of this study - result in predicted net count rates exceeding 875 kcpm for NaI-based survey meters or 100 kcpm for the pancake GM probe. These limitations on radiological triage screening are indicated in the handbooks for both their data tables and graphs. For the tables, data entries that exceed these maximum count rates are shaded by their corresponding distance-coded color. For the corresponding data plots, dashed horizontal lines are shown at 875 kcpm for NaI detectors or at 100 kcpm for the GM probe. When a given curve rises above the horizontal maximum count rate level, those combinations of elapsed time, detector position, and screening distance should be avoided, and another position or distance should be chosen for improved confidence in the screening measurement.

Recommendations for medical response based on estimated range of effective dose

Table 7 presents suggested medical responses given initial estimates of the range of effective dose, which in turn may be based on either portable survey meter measurements as described in this study, or more confirmatory measurements using traditional whole-body counters or special-purpose nuclear medicine gamma-camera scans. Guidance on the latter method can be found on the CDC Radiation Studies Branch homepage (see http://emergency.cdc.gov/radiation).

Four *Radiological Triage Conditions* are defined in Table 7 corresponding to estimated effective doses of below 50 mSv (Condition I), between 50 and 250 mSv (Condition II), between 250 and 500 mSv (Condition III), and exceeding 500 mSv (Condition IV). For each radionuclide and triage condition, various medical recommendations are given as indicated in footnotes A through Mof Table 7. For example, if the survey meter count rate

[1]Personal communication with Randal Stevens, Ludlum Measurements, Inc., Sweetwater, Texas (February 20, 2008).

measurement is made within 30–60 minutes of exposure, then two suggestions are given in Footnote A: (1) perform nasal swab if the intake is by inhalation, or (2) perform gastric lavage if the intake is by ingestion and the estimated effective dose exceed 50 mSv. If the effective dose is below 50 mSv, then the individual should be followed by their primary care physician for routine cancer screening (Footnote K). If the effective dose is above 50 mSv, then confirmatory measurements should be made via subsequent whole-body counting or gamma-camera scans (Footnote M). Other recommendations are given regarding the potential use of chelation therapy agents as per FDA guidance (www.fda.gov), as well as guidance to be given in a forthcoming revision to NCRP Report No. 65.

DISCUSSION

Representative example of handbook use by first responders

Consider a first responder using the Ludlum 12S to make rapid radiological triage decisions for a potentially contaminated adult female following a ^{60}Co inhalation exposure (5 μm AMAD / Type M). According to the data of Table 6 (from Handbook F, Table F6), the initial screening can be performed at either 100 cm or 200 cm from the subject without concern that the 875 kcpm maximum count rate for detector saturation would be exceeded (assuming the screening is performed in a moderate to low background environment). At one day following the incident, net count rates corresponding to 50, 250, and 500 mSv effective dose would be approximately 3.45, 17.2, and 34.5 kcpm, respectively, if measured with the subject facing the screener at 200 cm distance, and they would be approximately 2.26, 11.3, and 22.6 kcpm, respectively, if measured from the back of the subject at that same distance (see Table 6). The measured net count rate for the Ludlum 12S, with the subject either facing toward or away from the screener, can then be compared to these three count rate thresholds to determine which of the four radiological triage conditions would most likely apply for this subject. If the count rates are much below the 875 kcpm limit, the screener should repeat the measurement at a closer distance of 100 cm and confirm the original selection of triage condition.

Confirmatory measurements could continue with measurements make closer to the subject at either 30 cm or even 6 cm from the body surface using Table 5 data. However, as indicated by the shaded entries in this table, problems may arise when measurements are taken within 18 hours of exposure at a distance of 30 cm, or within 4 days of exposure at a distance of 6 cm. For example, it is estimated that if the individual retains sufficient ^{60}Co to yield an effective dose exceeding 500 mSv, then the 875 kcpm detector count rate maximum will likely be exceeded for either a AP chest or AP abdomen measurement at 30 cm if performed sooner than 18 hours following the acute inhalation event. Similar restrictions are noted for 6-cm screening measurements if the individual's effective dose exceeds 250 mSv and measurements are made within 3–4 days of exposure. Note, however, that earlier screening measurements at the 250 mSv dose level can be made at a screening distance of 6 cm if those measurements are made with the subject facing away from the screener (e.g., non-shaded entries in the upper portion of Table 5 for PA chest and PA abdomen positions). Here, the 875 kcpm is not expected to be exceeded provided that at least 4 hours have elapsed for a 6-cm PA chest measurement, and that at least 10 hours has elapsed for a 6-cm PA abdomen measurement. In such cases, however, it is strongly advisable to consider screening the individual either at greater distances (100 or 200 cm) to avoid these complications of detector saturation and/or reading misinterpretation.

As discussed below, there can be modest to large uncertainties in these values due to lack of knowledge of the particle size, the lung fluid solubility, and time since exposure. More importantly perhaps is the fact that the threshold values given in Tables 5 and 6 correspond to a single anatomical model of the adult female (60 kg total mass / 163 cm total stature)

whose cesium metabolism is assumed to exactly following ICRP reference biokinetics. Either of these conditions – the real subject's body morphometry and her true cesium biokinetics – can potentially differ substantially from the reference conditions assumed in this study. Nevertheless, the count rate thresholds given in Tables 5 and 6 (and in the corresponding Handbooks) can be used to determine, not the true value of the individual's effective dose, but whether that effective dose most likely lies above or below 50, 250, or 500 mSv defining the four radiological triage conditions of Table 7. Only confirmatory measurements made via whole-body counting, gamma-camera screening, or bioassay analysis can be used to assess a single estimate of the individual's effective dose. The survey meter readings give only an indication of the dose range.

Variations in count rate threshold by detector type

In Figure 7A to 7E, we display time-dependent detector count rate thresholds corresponding to a 250 mSv effective dose to the reference adult male as screened in the AP chest position at 30 cm distance. Each figure corresponds to a given radionuclide of a particle size distribution and lung solubility class as indicated in the figure caption. In all cases, the most sensitive detector is shown to be the Ludlum 375-0 (3" by 1" NaI crystal), while the least sensitive detector, by more than 1 to 2 orders of magnitude, is the Ludlum 44-9 pancake GM probe. As a result, CDC Handbooks G and H recommend that this detector not be used at all for ^{241}Am screening, and that for the other radionuclides, only screening distances 6 cm and 30 cm be considered.

For the scenarios selected, the GM probe values never exceed their maximum count rate of 100 kcpm. However, the maximum count rate of 875 kcpm for the Ludlum 375-0 is shown to be exceeded during screening times less than 1 day post-intake for both ^{60}Co and ^{137}Cs inhalation exposures (Fig. 7B and 7C), and for screening times less than ~5 hours post-intake for ^{131}I inhalation exposures (Fig. 7D). For ^{192}Ir exposures (Fig. 7E), the 30-cm AP chest measurement cannot be performed using the relatively sensitive Ludlum 375-30 waste monitor, and either another detector should be used for this case, or the screening should be conducted at a greater distance (e.g., 200 cm). Count rates for ^{241}Am exposure screening are shown to be very low (Fig. 7A), and thus the optimal detector of the four presented here would be the Ludlum 375-30. Other more viable options for rapid ^{241}Am screening would be the use of a dual-scintillator phoswich detector (not yet considered by our study group). Very comparable results are shown for the Ludlum 44-17 scintillator probe and the Ludlum 12S survey meter for both ^{131}I and ^{192}Ir inhalation exposures (Fig. 7D and 7E), with a slightly higher sensitivity shown for the 12S over the 44-17 in the case of ^{60}Co and ^{137}Cs. For these two higher-energy radionuclides, the significantly thicker crystal for the former (1 inch versus 1 mm) more than compensates for the smaller detector diameter (1 inch versus 2 inches). For ^{241}Am inhalation exposure screening, the Ludlum 44-17 is shown to yield higher count rates for the same 250 mSv effective dose in comparison to those seen for the Ludlum 12S (Fig. 7A).

Variations in count rate threshold by detector position and distance

Figures 5 and 6 provide representative examples of how the count rate threshold for a given detector (e.g., Ludlum 12S) and a given effective dose varies with both detector anatomical position (chest versus abdomen, or AP versus PA) and screening distance (6, 30, 100, and 200 cm). At close distances (e.g., 6 cm), significant differences are noted between chest and abdomen screening positions, more so for the AP positions (Fig. 5A) than for the PA positions (Fig. 5B). Furthermore, the time-dependence of these count rate thresholds is enhanced at 6 cm in comparison to values at larger distances. Differences in chest versus abdomen detector count rate thresholds diminish with distance as expected, and at a distance of 200 cm, are statistically indistinguishable in the Monte Carlo simulation results. In

comparing pairs of graphs for AP versus PA screening at each distance, it is noted that higher detector count rates are seen at a given effective dose in the AP screening position than in the PA screening position. This can, on occasion, be of use in avoiding detector saturation. For example, modeling results indicate that ^{60}Co screening in the AP positions at 30 cm (Fig. 5C) would result in detector saturation if the individual's intake resulted in an effective dose approaching 500 mSv and the screening was performed within 1 day of exposure. However, the 500 mSv dose level may be screened for at all times post-intake if the individual were simply asked to face away from the detector during the measurement (data of Fig. 5D).

Variations in count rate threshold by particle size and lung fluid solubility

In most RDD exposure events, reasonable estimates can be made of the elapsed time since exposure, while spectral analyses can be used to properly identify the radionuclide involved. However, detailed knowledge of the particle size distribution and/or the lung fluid solubility of the inhaled material will most likely not be known at the time of emergency screening. Consequently, it is instructive to understand the variability in detector count rate thresholds with changes in both these parameters, as this uncertainty may possibly result in a misidentification of the Table 7 triage condition.

In Figure 8, detector count rates thresholds for an effective dose of 250 mSv are given for all six inhalation exposure scenarios and one ingestion scenario for ^{192}Ir. The data equate to an adult female subject screened at 200 cm in the AP position via a Ludlum 12S survey meter. For each of solubility types (S, M, and F), count rate thresholds are shown to higher for a 5-μm AMAD distribution than for 1-μm AMAD distribution out to ~3 days for Type F materials (after which the count rates do not differ strongly with particle size), and out to ~5 days for Type M and S materials (after which count rates are lower for the larger particle size distribution). Correspondingly, Type F aerosols of ^{192}Ir are shown to have a much higher count rate threshold than for either Type M or S aerosols at the same particle size distribution. A much more pronounced change in count rate threshold is shown for an ingestion exposure, thus highlighting the importance of ascertaining the intake route.

If the exposure to ^{192}Ir is known to be an acute inhalation, the lack of knowledge regarding particle size and solubility will force one to assume a standard set of aerosol characteristics – such as a 1-μm AMAD distribution of Type M solubility. The data of Table 8 then gives the range of errors that could be made in determining whether or not the subject's effective dose exceeds or is below 250 mSv. If the particle size is correctly chosen (1-μm AMAD), but the solubility type is in fact Type F or Type S, then the count rate threshold will be a factor of ~2.5 to 4.0 too low for true Type F aerosols, but will be only 20–25% too high for true Type S aerosols. If the solubility type is correctly chosen as Type M, but the aerosol is in fact of a 5-μm AMAD size distribution, count rate threshold will be a factor of 2 too low at short times to values ~18% too high at longer times post-intake. Errors up to a factor of ~4 are shown if both the size and solubility class are incorrectly estimated (e.g., 5-μm AMAD and Type F). The data of both Table 8 and Figure 8 indicate that this default set of aerosol characteristics (1-μm AMAD and Type M) would tend to result in conservative assignments of Triage Condition III (250–500 mSv) when in fact Triage Condition II (50–250 mSv) might have been selected had the true particle size and solubility been known. This is true for all by one of the possible incorrectly selected exposure scenarios (1-μm Type S aerosols where the threshold net count rate is ~20% lower than the assumed default curve).

Variations in count rate threshold by subject gender

It is also instructive to see to what extent separate tables for the adult male and adult female should be given. In Figure 9, we show net count rate thresholds for a 250 mSv effective dose

for both adult genders as a function of time and screening distance for ^{131}I ingestions exposures (screened in the AP chest position with the Ludlum 12S). As expected, the smaller frame and mass of the adult female results in less internal photon absorption and scatter with a correspondingly higher detector count rate for a given 250 mSv effective dose. Gender differences are shown to be enhanced both at the shorter screening distances, and correspondingly minimized at greater distances. As shown in Table 9, ratios of the female to male detector thresholds vary from a high of 1.88 at 6 cm (0.4 days) to a low of 1.05–1.07 at 200 cm (minutes following exposure and then at times beyond ~4–5 days post-intake).

CONCLUSIONS

In situations where relatively large numbers of potentially contaminated individuals must be screened following a radiological terrorist event, simple and easily implemented methods of radiological triage must be employed by first responders, first receivers, and/or in-field medical personal. In this study, the use of hand-held portable survey meters, either NaI-based or GM-based, was explored for five radionuclides of potential use in an RRD device: ^{241}Am, ^{60}Cs, ^{137}Cs, ^{131}I, and ^{192}Ir. Both ingestion and inhalation exposure scenarios, were considered, with the latter including a sensitivity study on particle size and lung fluid solubility. Two hybrid computational phantoms – one male and one female, each representing the ICRP 89 reference adults – were used to simulate the time-dependent organ burdens and the corresponding detector net count rates corresponding to intakes resulting in either a 50, 250, or 500 mSv committed effective dose. Four detector positions were considered – AP chest, AP abdomen, PA chest, and PA abdomen, as well as four detector-to-body surface distances – 6, 30, 100, and 200 cm. Values of net count rate thresholds are provided for each dose level as a function of time post-intake for all combinations of detector position and distance. The data are given in both graphical and tabular format in a series of eight Handbooks available at the CDC Radiation Studies Branch website: (see http://emergency.cdc.gov/radiation). It is not the intent of this document nor the CDC handbooks to suggest the use of portable survey meters to assign a definitive value of the effective dose to a given screened individual. Rather, the data are intended to be used to assign the screened individual to one of four possible dose ranges (<50, 50–250, 250–500, and >500 mSv) with resultant recommendations given on potential therapeutic interventions, and radiological as well as medical follow-up.

The count rate data provided in the CDC handbooks documented in this study are subject to a variety of uncertainties. The Monte Carlo modeling of this study assumed that both the adult male and adult female subject were of ICRP 89 reference body morphometries, and that each radionuclide was metabolized according to its reference biokinetic model given by the ICRP. Use of handbook tables and graphs to assign the radiological triage condition presumes knowledge of the radionuclide involved and the time interval between intake and survey meter screening. Furthermore, knowledge of the particle size distribution and the lung fluid solubility would be helpful, but if not known, use of default aerosol characteristics (1-μm AMAD and Type M solubility class) will tend to result in a conservative assignment of the dose range and radiological triage conditions (I, II, III, or IV), as count rate thresholds will typically be higher that those given for 1-μm Type M aerosols at a given effective dose. Future studies will consider both underweight and overweight adults, as well as children of various ages and body sizes (Lee *et al*. 2007; Lee *et al*. 2008), which are both easily accommodated via hybrid phantom technology. These extensions will thus allow for refinements in the survey meter screening methodology presented here so as to cover the full range of individuals potentially exposed following an RDD terrorist event.

Acknowledgments

This work was performed under contract TKC 30-06 16601 CDC Task 29 with TKC Integration Services, Inc. and the U.S. Centers for Disease Control and Prevention. The authors wish to thank the following individuals at Ludlum Measurements, Inc. for the very help discussions of detector response and for providing schematics for MCNP model construction: Dwane Stevens, Jamie Witt, Chris Cudd, Dwane Watts, and Randall Stevens. In addition, the authors wish to acknowledge the assistant of Dr. Ronald Goans and Dr. Albert Wiley for their review of the radiological triage recommendations given in this paper.

This work was supported by the TKC Integration Services, Inc.

References

Bolch WE, Hurtado JL, Lee C, Manger R, Hertel N, Dickerson W. Guidance on the use of hand-held survey meters for radiological triage: Time-dependent detector count rates correspondign to 50, 250, and 500 mSv effective dose for adult males and adult females. Health Phys. this issue.

Eckerman, KF.; Endo, A. MIRD: Radionuclide Data and Decay Schemes. 1st ed.. Eckerman, KF.; Brill, AB.; Howell, RW., editors. Reston, VA: The Society of Nuclear Medicine; 2008.

Harper FT, Musolino SV, Wente WB. Realistic radiological dispersal device hazard boundaries and ramifications for early consequence management decisions. Health Phys. 2007; 93:1–16. [PubMed: 17563488]

ICRP ICRP Publication 66: Human respiratory tract model for radiological protection. Ann ICRP. 1994; 24:1–482.

ICRP Age-dependent doses to members of the public from intake of radionuclides: Part 5-compilation of ingestion and inhalation dose coefficients. ICRP Publication. Vol. 72. Elmsford, New York: International Commission on Radiological Protection; 1996.

ICRP Database of dose coefficients: workers and members of the public (ICRP Publication 72) [CD-ROM]. International Commission on Radiological Protection; 2002.

Lee C, Lee C, Lodwick D, Bolch WE. NURBS-based 3D anthropometric computational phantoms for radiation dosimetry applications. Radiat Prot Dosim. 2007; 127:227–232.

Lee C, Lodwick D, Williams JL, Bolch WE. Hybrid computational phantoms of the 15-year male and female adolescent: applications to CT organ dosimetry for patients of variable morphometry. Med Phys. 2008; 35:2366–2382. [PubMed: 18649470]

NCRP Management of persons accidentally contaminated with radionuclides. Vol. 65. Bethesda, MD: National Council on Radiation Protection and Measurements; 1980. Report No

NCRP Management of terrorist events involving radioactive material. Vol. 138. Bethesda, MD: National Council on Radiation Protection and Measurements; 2001. Report No

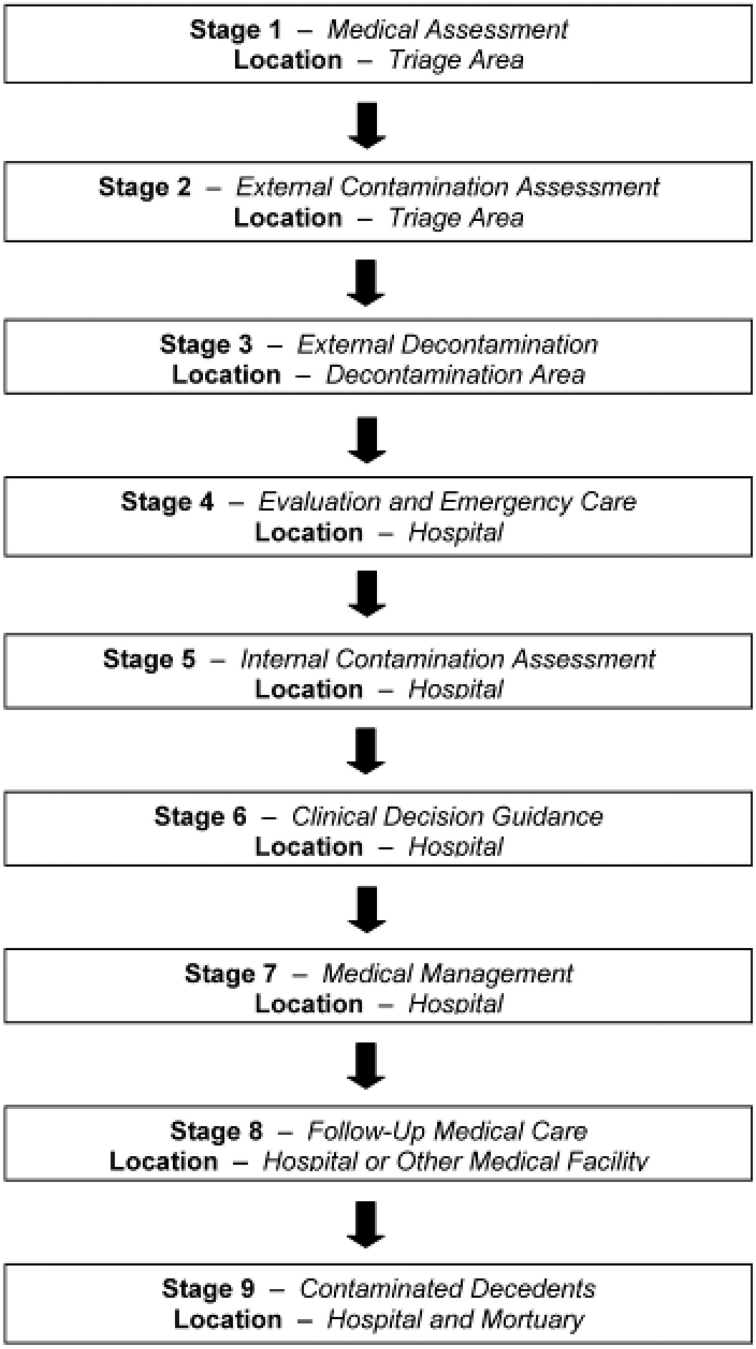

Figure 1.
Stages in the medical management of contaminated individuals.

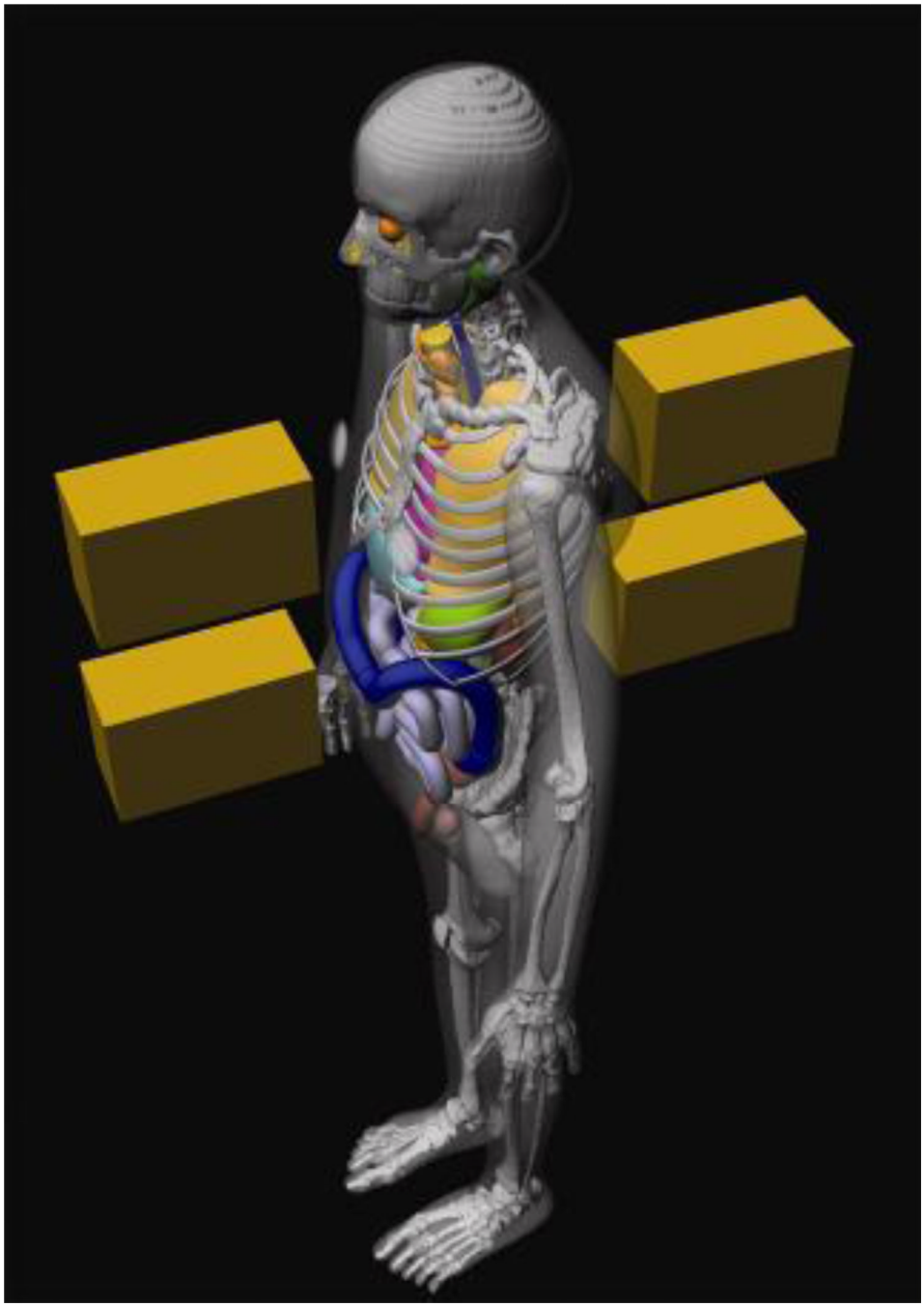

Figure 2.
Representative schematic of the four detector positions – AP chest, AP Abdomen, PA Chest, and PA Abdomen – applied the adult male hybrid phantom.

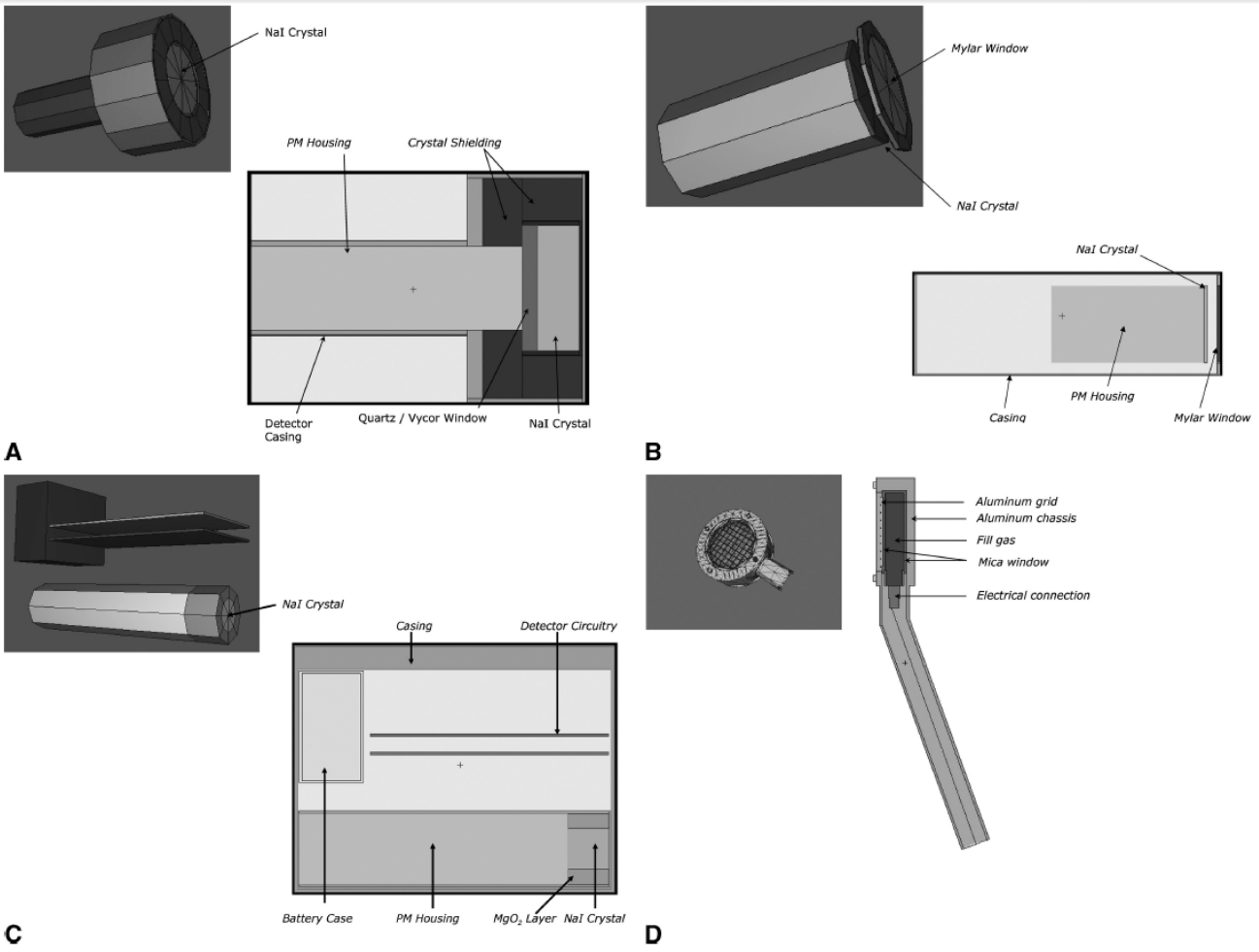

Figure 3.
MCNP schematic drawings of the four survey meters considered in this study: **(A)** Ludlum 375-30 waste monitor, **(B)** Ludlum 44-17 low-energy gamma scintillator, **(C)** Ludlum 12S survey meter, and **(D)** Ludlum 44-9 pancake GM probe.

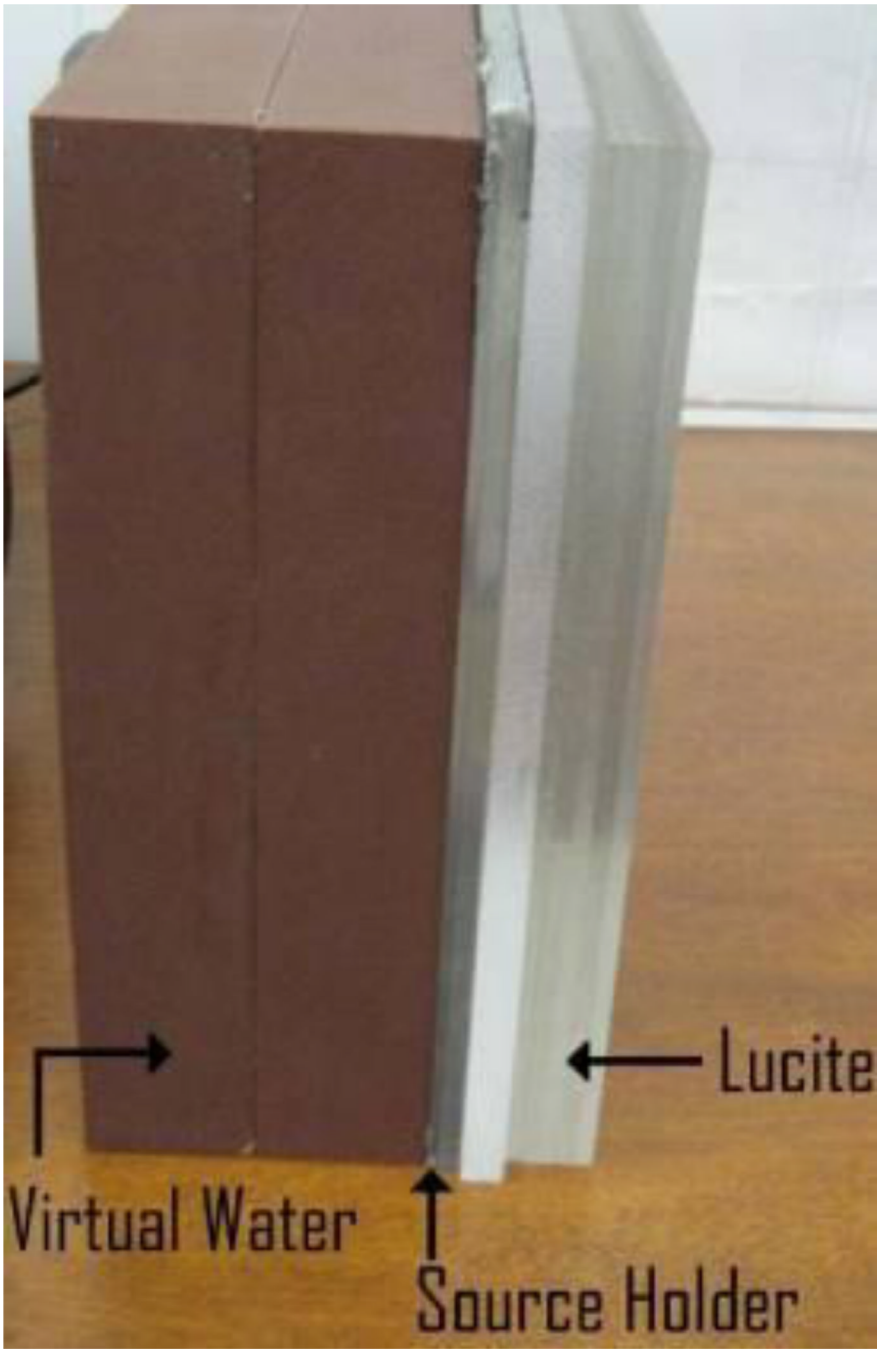

Figure 4.
Lucite slab phantom used to derive MCNP tally correction factors for the Ludlum 44-9 GM probe.

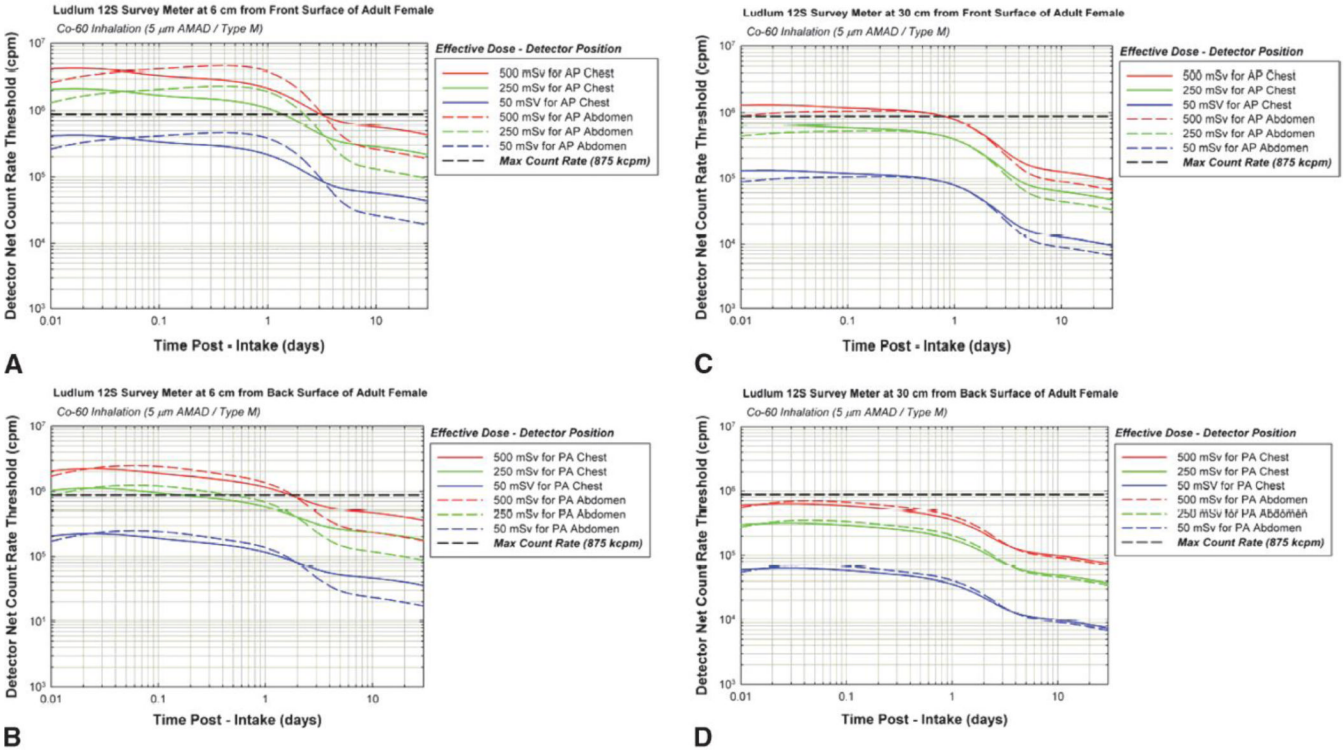

Figure 5.

Representative graphs from Handbook F on the use of the Ludlum 12S survey meter for radiological triage screening of an adult female subject at distances of either 6 cm (plots on the left) or 30 cm (plots on the right). Exposure scenario: acute inhalation of ^{60}Co aerosol at 5 μm AMAD and solubility class Type M.

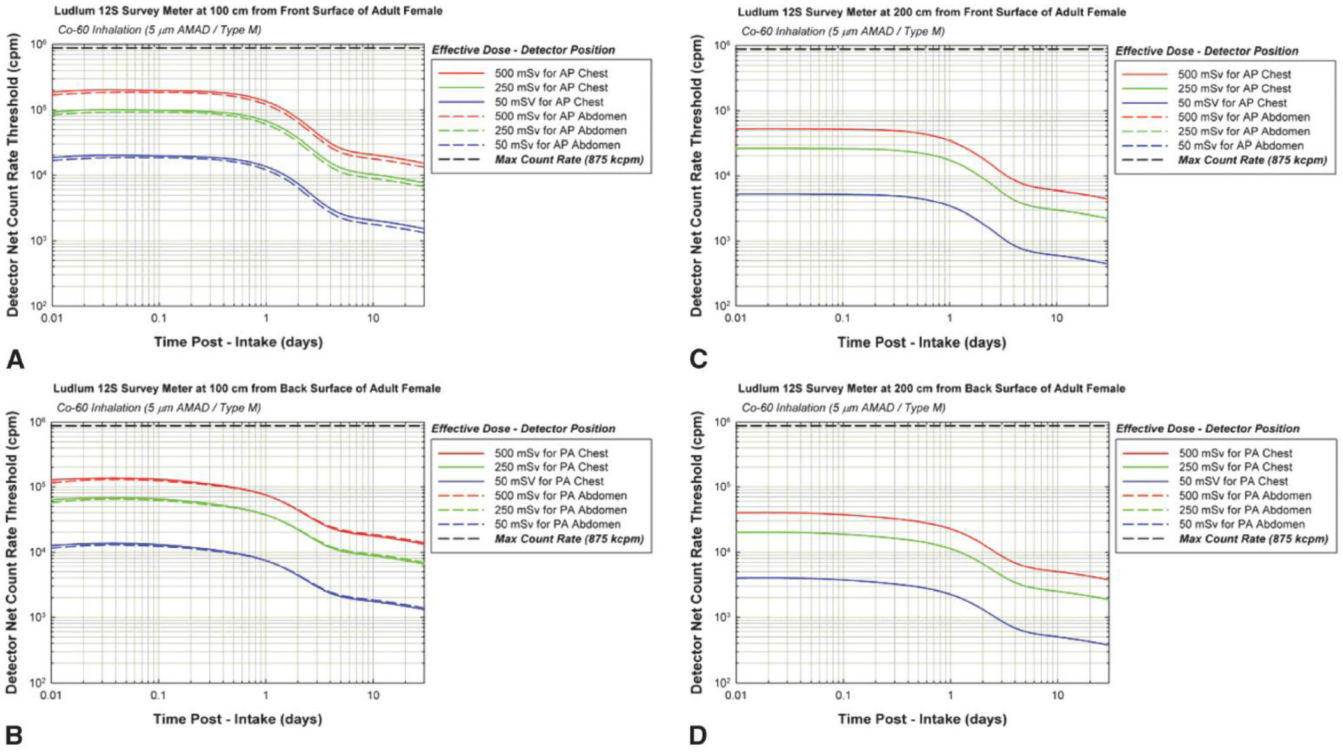

Figure 6.

Representative graphs from Handbook F on the use of the Ludlum 12S survey meter for radiological triage screening of an adult female subject at distances of either 100 cm (plots on the left) or 200 cm (plots on the right). Exposure scenario: acute inhalation of ^{60}Co aerosol at 5 μm AMAD and solubility class Type M.

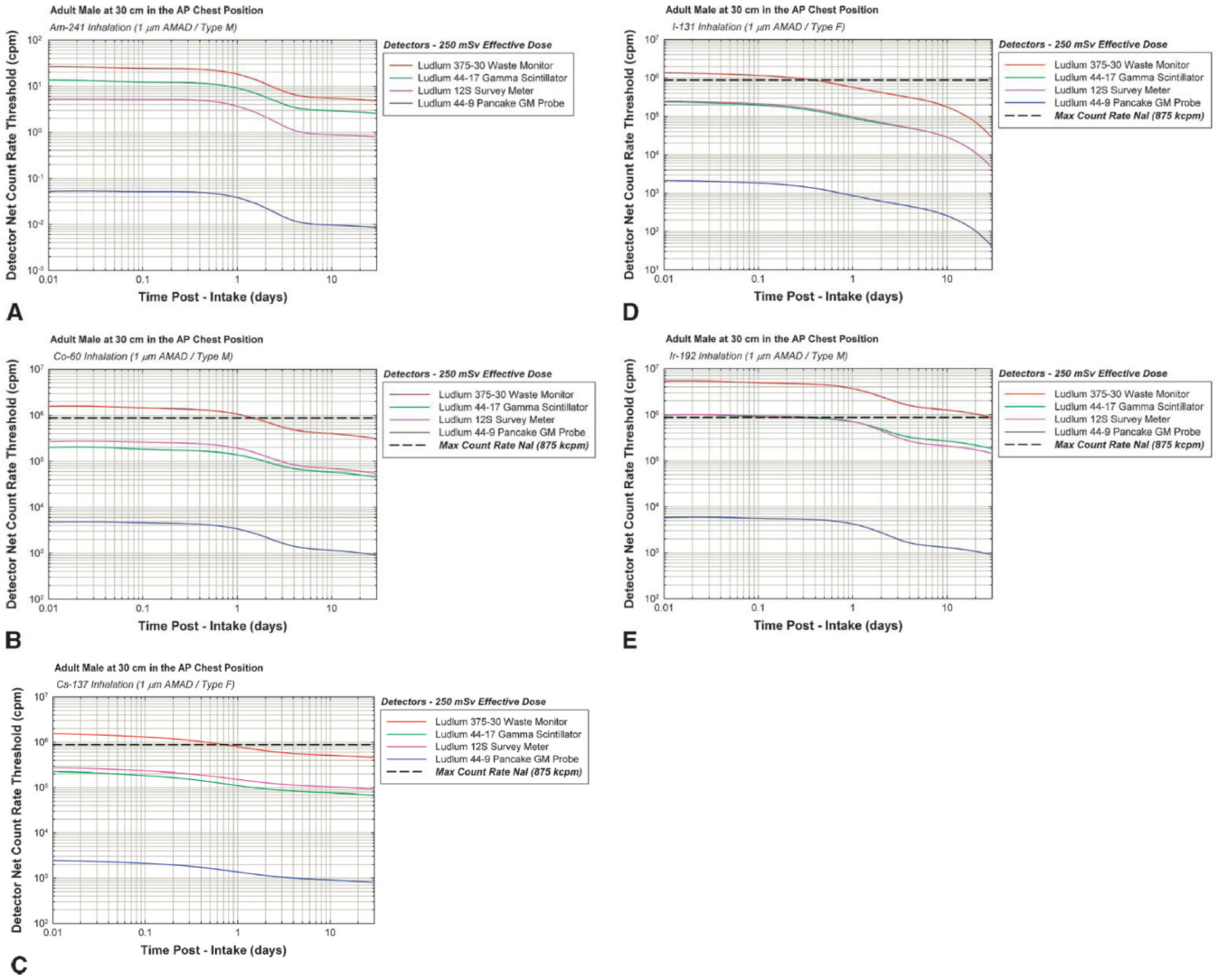

Figure 7.

Comparison of 250 mSv count rate thresholds for the four survey meters for each of five radionuclide exposure scenarios: **(A)** ^{241}Am inhalation (1-μm AMAD / Type M), **(B)** ^{60}Co inhalation (1-μm AMAD / Type M), **(C)** ^{137}Cs inhalation (1-μm AMAD / Type F), **(D)** ^{131}I inhalation (1-μm AMAD / Type M), and **(E)** ^{192}Ir inhalation (1-μm AMAD / Type M). As plots correspond to the reference adult male screened in the AP chest position at 30 cm distance

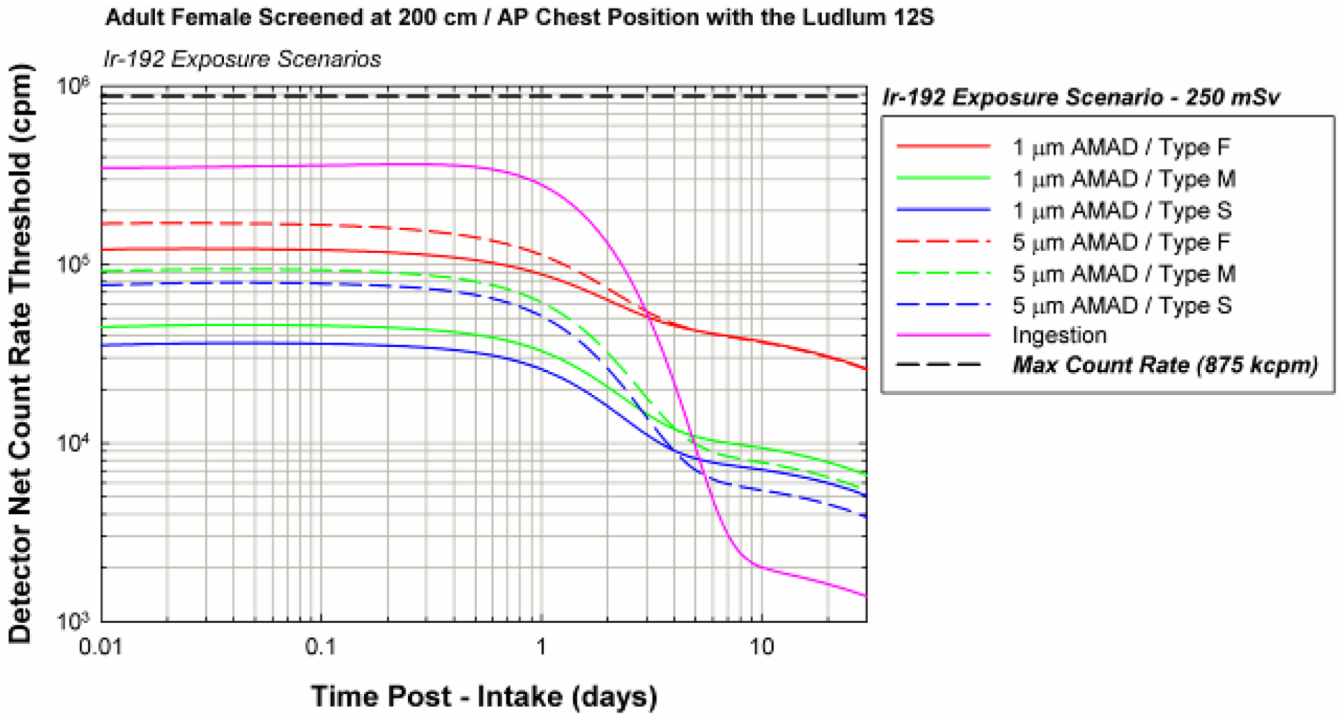

Figure 8.

Time-dependent detector count rate thresholds corresponding to an effective dose of 250 mSv for six different inhalation and one ingestion exposure scenario involving ^{192}Ir. Values correspond to an adult female screened in the AP direction at 200 cm using a Ludlum 12S survey meter. Corresponding ratios to a reference inhalation exposure (1-μm AMAD / Type M) are given in Table 8.

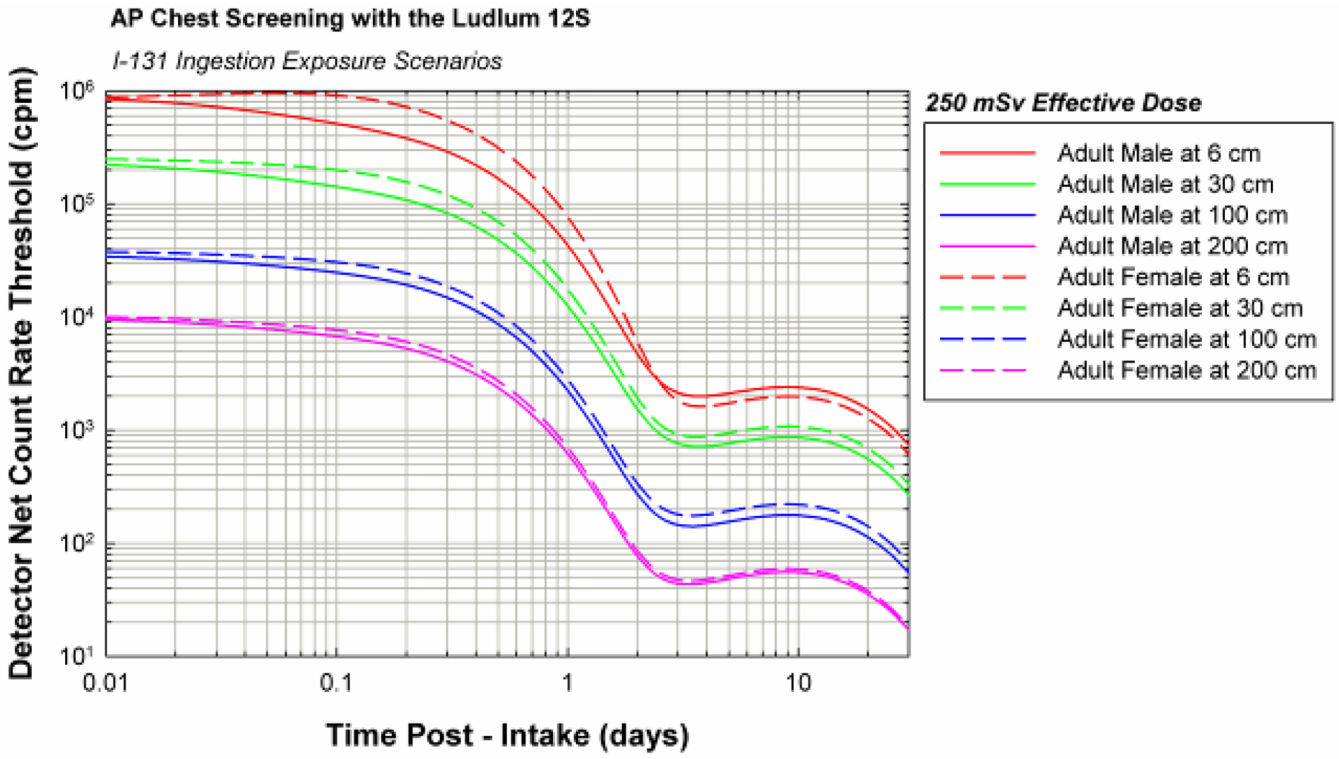

Figure 9.
Time-dependent detector count rate thresholds corresponding to an effective dose of 250 mSv following ingestion of ^{131}I for both an adult male (solid curves) and an adult female (dashed curves). Both are screened in the AP chest position using a Ludlum 12S survey meter at distances of 6, 30, 100, or 200 cm.

Table 1

Summary of dose coefficients for both Effective Dose and Organ Equivalent Dose (Sv per Bq intake) for all 21 exposure scenarios considered in this study.

Exposure				Solubility		Effective dose	Equivalent dose 30 days to lungs	Equivalent dose 30 days to RBM	Equivalent dose 30 days to thyroid
Scenario	Radionuclide	Intake	AMAD	Class	f_A	(Sv/Bq-intake)	(Sv/Bq-intake)	(Sv/Bq-intake	(Sv/Bq-intake)
1	Am-241	Inhal	1 μm	Type M	0.0005	3.90×10^{-5}	1.70×10^{-5}	7.20×10^{-8}	
2	Am-241	Inhal	5 μm	Type M	0.0005	2.70×10^{-5}	1.30×10^{-5}	7.40×10^{-8}	
3	Am-241	Inges			0.0005	2.00×10^{-7}	3.50×10^{-11}	1.20×10^{-9}	
4	Co-60	Inhal	1 μm	Type M	0.10	9.60×10^{-9}	1.90×10^{-8}	6.60×10^{-10}	
5	Co-60	Inhal	1 μm	Type S	0.05	2.90×10^{-3}	2.20×10^{-8}	6.90×10^{-10}	
6	Co-60	Inhal	5 μm	Type M	0.10	7.10×10^{-9}	1.50×10^{-8}	5.60×19^{-10}	
7	Co-60	Inhal	5 μm	Type S	0.05	1.70×10^{-8}	1.70×10^{-8}	5.40×10^{-10}	
8	Co-60	Inges			0.10	3.40×10^{-9}	2.10×10^{-10}	5.70×10^{-10}	
9	Cs-137	Inhal	1 μm	Type F	1.00	4.80×10^{-9}	8.00×10^{-10}	8.00×10^{-10}	
l0	Cs-137	Inhal	5 μm	Type F	1.00	6.70×10^{-9}	1.10×10^{-9}	1.10×10^{-9}	
11	Cs-137	Inges			1.00	1.30×10^{-8}	2.20×10^{-9}	2.30×10^{-9}	
12	I-131	Inhal	1 μm	Type F	1.00	7.60×10^{-9}	5.70×10^{-11}		1.40×10^{-7}
12	I-131	Inhal	5 μm	Type F	1.00	1.10×10^{-8}	7.80×10^{-11}		2.00×10^{-7}
14	I-131	Inges			1.00	2.20×10^{-8}	9.70×10^{-11}		4.00×10^{-7}
15	Ir-192	Inhal	1 μm	Type F	0.01	1.80×10^{-9}	4.50×10^{-10}	4.50×10^{-10}	
16	Ir-192	Inhal	1 μm	Type M	0.01	4.90×10^{-9}	2.10×10^{-8}	2.50×10^{-10}	
17	Ir-192	Inhal	1 μm	Type S	0.01	6.20×10^{-9}	2.40×10^{-8}	2.30×10^{-10}	
18	Ir-192	Inhal	5 μm	Type F	0.01	2.20×10^{-9}	5.40×10^{-10}	5.20×10^{-10}	
19	Ir-192	Inhal	5 μm	Type M	0.01	4.10×10^{-9}	1.70×10^{-8}	2.20×10^{-10}	
20	Ir-192	Inhal	5 μm	Type S	0.01	4.90×10^{-9}	2.00×10^{-8}	1.90×10^{-10}	
21	Ir-192	Inges			0.01	1.40×10^{-9}	3.20×10^{-11}	1.90×10^{-10}	

Table 2

Source organs and tissues modeled in the computational phantoms for each of the five radionuclides considered in this study. Organs for which the fractional uptake never exceeds 1% were not considered in modeling survey meter response functions.

Source tissue	Am-241	Co-60	Cs-137	Cs-137	Ir-192
ET1	✓	✓	✓	✓	✓
ET2	✓	✓	✓	✓	✓
Trachea & lungs	✓	✓	✓	✓	✓
Stomach contents	✓	✓	✓	✓	✓
Small intestine content	✓	✓	✓	✓	✓
Blood	✓	✓	✓	✓	✓
Left colon content	✓	✓	✓	✓	✓
Right colon content	✓	✓	✓	✓	✓
Liver	✓	✓			✓
Other tissues	✓	✓	✓	✓	✓
Skeleton	✓				
Kidneys	•				•
Testes	•				
Ovaries	•				
Thyroid				✓	
Spleen					•
Urinary bladder	•	•	•	•	•

Note: Other Tissues are defined as all soft tisuses of the phantom excluded those listed above.

Note: Dots indicate tissues with uptake fractions never exceeding 1%.

Table 3

Selection of source tissues and organs in the computational phantoms used to model radionuclide sources within circulating blood of the adult male or female.

Blood sources - ICRP publication 89			Blood sources - present study		
Organ or tissue	**Male (%)**	**Female (%)**	**Organ or tissue in phantom**	**Male (%)**	**Female (%)**
Fat	5.00	8.51	Residual soft tissues	46.90	46.90
Brain	1.20	1.20	Brain	1.20	1.20
Stomach/esophagus	1.00	1.00	Small intestine wall	3.80	3.80
Small intestine	3.80	3.80	Colon	2.20	2.20
Colon	2.20	2.20	Heart content	9.00	9.00
Right heart content	4.50	4.50	Heart wall	LOO	LOO
Left heart content	4.50	4.50	Kidneys	2.00	2.00
Coronary tissue	1.00	1.00	Liver	10.00	10.00
Kidneys	2.00	2.00	Lungs	12.50	12.50
Liver	10.00	10.00	Skeleton	7.00	7.00
Pulmonary tissues	10.50	10.50	Skin	3.00	3.00
Bronchial tissues	2.00	2.00	Spleen	1.40	1.40
Skeletal muscle	14.00	10.51			
Pancreas	0.60	0.60			
Skeleton					
Red marrow	4.00	4.00			
Trabecular bone	1.20	1.20			
Cortical bone	0.80	0.80			
Other skeleton	1.00	LOO			
Skin	3.00	3.00			
Spleen	1.40	1.40			
Thyroid	0.06	0.06			
Lymph nodes	0.20	0.20			
Gonads	0.04	0.02			
Adrenals	0.06	0.06			
Urinary bladder	0.02	0.02			
All other tissues	1.92	1.92			

Blood sources - ICRP publication 89			Blood sources - present study		
Organ or tissue	**Male (%)**	**Female (%)**	**Organ or tissue in phantom**	**Male (%)**	**Female (%)**
Aorta and large veins	6.00	6.00			
Large veins	18.00	18.00			
	100.00	100.00		100.00	100.00

Table 4

List of radiological triage screening handbooks available at the CDC website for its Radiation Studies Branch.

Handbook	Survey meter	Screened subject
A	Ludlum 365-30 waste monitor	Reference adult male
B	Ludlum 365-30 waste monitor	Reference adult female
C	Ludlum 44-17 gamma scintillator	Reference adult male
D	Ludlum 44-17 gamma scintillator	Reference adult female
E	Ludlum 12S survey meter	Reference adult male
F	Ludlum 12S survey meter	Reference adult female
G	Ludlum 44-9 pancake GM probe	Reference adult male
H	Ludlum 44-9 pancake GM probe	Reference adult female

Table 5

Representative table from Handbook F on the use of the Ludlum 12S survey meter for radiological triage screening of the aduit female at distances of 6 and 30 cm. Exposure scenario 6: acute inhalation of ^{60}Co aerosol at 5 μm AMAD and solubility class Type M.

Time Since Intake		Ludlum 12S Survey Meter (Distance from Surface of 50th Percentile Adult Female; 6 cm)											
		Nat Count Rate (cpm) for 50 mSv ED				Nat Count Rate (cpm) for 250 mSv ED				Nat Count Rate (cpm) for 500 mSv ED			
Time (days)	Time (hours)	AP Chest	AP Abdomen	PA Chest	PA Abdomen	AP Chestt	AP Abdomen	PA Chest	PA Abdomen	AP Chest	AP Abdomen	PA Chest	PA Abdomen
	0.5	4.24E+05	3.34E+05	2.24E+05	2.20E+05	2.12E+06	1.67E+06	1.12E+06	1.10E+06	4.24E+06	8.34E+06	2.24E+06	2.20E+06
	1	3.94E+05	3.78E+05	2.17E+05	2.46E+05	1.97E+06	1.89E+06	1.09E+06	1.23E+06	3.94E+06	3.78E+06	2.17E+06	2.46E+06
	2	3.47E+05	4 08E+05	1.95E+05	2.47E+05	1.74E+06	2.04E+06	9.77E+05	1.23E+06	3.17E+06	4.34E+06	1.85E+06	2.47E+06
	4	3.16E+05	4.40E+05	1.74E+05	2.24E+05	1.58E+06	2.20E+06	8.72E+05	1.12E+06	3.16E+06	4.40E+06	1.74E+06	2.24E+06
	6	3.04E+05	4.57E+05	1.64E+05	2.05E+05	1.52E+06	2.29E+06	8.19E+05	1.02E+06	3.04E+06	4.57E+06	1.54E+06	2.05E+06
	8	2.95E+05	4.65E+05	1.56E+05	1.91E+05	1.47E+06	2.32E+06	7.80E+05	9.56E+05	2.95E+06	4.65E+06	1.56E+06	1.91E+06
	10	2.85E+05	4.66E+05	1.50E+05	1.81E+05	1.43E+06	2.33E+06	7.48E+05	9.06E+05	2.85E+06	4.66E+06	1.50E+06	1.81E+06
	12	2.75E+05	4.62E+05	1.44E+05	1.73E+05	1.38E+06	2.31E+06	7.19E+05	8.67E+05	2.85E+06	4.62E+06	1.44E+06	1.73E+06
	14	2.65.E+05	4.54E+05	1.39E+05	1.67E+05	1.33E+06	2.27E+06	6.93E+05	8.34E+05	2.65E+06	4.54E+06	1.39E+06	1.67E+06
	16	2.55E+05	4.42E+05	1.34E+05	1.60E+05	1.27E+06	2.21E+06	6.69E+05	8.02E+05	2.55E+06	4.42E+06	1.34E+06	1.60E+06
	18	2.45E+05	4.Z9E+05	1.29E+05	1.54E+05	1.22E+06	2.15E+06	6.45E+05	7.72E+05	2.45E+06	4.29E+06	1.29E+06	1.54E+06
	20	2.35E+05	4.14E+05	1.24E+05	1.48E+05	1.17E+06	2.07E+06	6.22E+05	7.42E+05	2.35E+06	4.14E+06	1.24E+06	1.48E+06
1		2.15E+05	3.82E+05	1.16E+05	1.37E+05	1.08E+06	1.91E+06	5.79E+05	6.83E+05	2.15E+06	3.82E+06	1.16E+06	1.37E+06
2		1.30E+05	1.99E+05	7.99E+04	1.81E+04	6.50E+05	9.95E+05	3.99E+05	3.31E+05	1.30E+06	1.99E+06	7.99E+05	7.81E+05
3		9.00E+04	9.98E+04	6.33E+04	4.80E+04	4.50E+05	4.99E+05	3.16E+05	2.40E+05	9.00E+05	9.98E+05	6.33E+05	4.80E+05
4		7.32E+04	5.72E+04	5.61E+04	3.50E+04	3.66E+05	2.86E+05	2.80E+05	1.75E+05	7.32E+05	5.72E+05	5.61E+05	3.50E+05
5		6.60E+04	3.99E+04	5.27E+04	2.95E+04	3.30E+05	2.00E+05	2.64E+05	1.48E+05	6.60E+05	3.99E+05	5.27E+05	2.95E+05
6		6.26E+04	3.28E+04	5.09E+04	2.70E+04	3.13E+05	1.64E+05	5.14F+04	1.35E+05	6.26E+05	3.28E+05	5.09E+05	2.70E+05
7		6.06E+04	2.96E+04	4.96E+04	2.57E+04	3.03E+05	1.48E+05	2.48E+05	1.28E+05	6.06E+05	2.96E+05	4.96E+05	2.57E+05
8		5.92E+04	2.80E+04	4.86E+04	2.48E+04	2.96E+05	1.40E+05	2.43E+05	1.24E+05	5.92E+05	2.80E+05	4.86E+05	2.48E+05
9		5.81E+04	2.69E+04	4.77E+04	2.41E+04	2.90E+05	1.3SE+05	2.39E+05	1.21E+05	6.81E+05	2.69E+05	4.77E+05	2.41E+05
10		5.70E+04	2.61E+04	4.69E+04	2.38E+04	2.85E+05	1.31E+05	2.34E+05	1.18E+05	5.70E+05	2.61E+05	4.69E+05	2.38E+05
15		5.30E+04	2.37E+04	4.36E+04	2.16E+04	2.85E+05	1.19E+05	2.18E+05	1.08E+05	5.30E+05	2.37E+05	2.36E+05	2.18E+05
20		4.90E+04	2.14E+04	4.03E+04	1.97E+04	2.45E+05	1.07E+05	2.02E+05	9.86E+04	4.90E+05	2.14E+05	4.03E+05	1.87E+05
25		4.61E+04	2.01E+04	3.79E+04	1.86E+04	2.30E+05	1.00E+05	1.90E+05	9.28E+04	4.61E+05	2.01E+05	3.79E+05	1.86E+05

Time Since Intake		Ludlum 12S Survey Meter (Distance from Surface of 50th Percentile Adult Female; 6 cm)											
		Nat Count Rate (cpm) for 50 mSv ED				Nat Count Rate (cpm) for 250 mSv ED				Nat Count Rate (cpm) for 500 mSv ED			
Time (days)	Time (hours)	AP Chest	AP Abdomen	PA Chest	PA Abdomen	AP Chestt	AP Abdomen	PA Chest	PA Abdomen	AP Chest	AP Abdomen	PA Chest	PA Abdomen
30		4.32E+04	1.88E+04	3.56E+04	1.74E+04	2.16E+05	9.38E+05	1.78E+05	8.70E+04	4.32E+056	1.88E+05	3.56E+05	1.74E+05

Time Since Intake		Ludlum 12S Survey Meter (Distance from Surface of 50th Percentile Adult Female: 30 cm)											
		Net Count Rate (cpm) for 50 mSv ED				Net Count Rate (cpm) for 250 mSv ED				Net Count Rate (cpm) for 500 mSv ED			
Time (days)	Time (hours)	AP Chest	AP Abdomen	PA Chest	PA Abdomen	AP Chest	AP Abdomen	PA Chest	PA >Abdomen	AP Chest	AP Abdomen	PA Chest	PA Abdomen
	0.5	1.32E+05	9.82E+04	6.30E+04	6.59E+04	6.59E+05	4.91E+05	3.15E+05	3.29E+05	1.32E+06	9.82E+05	6.30E+05	6.59E+05
	1	1.28E+05	1.03E+05	6.27E+04	6.99E+04	6.38E+05	5.16E+05	3.14E+05	3.50E+05	1.28E+06	1.03E+06	6.27E+05	6.99E+05
	2	1.21E+05	1.05E+05	5.96E+04	6.79E+04	6.04E+05	5.26E+05	2.98E+05	3.40E+05	1.21E+06	1.05E+06	5.96E+05	6.79E+05
	4	1.15E+05	1.07E+05	5.49E+04	6.27E+04	5.76E+05	5.33E+05	2.75E+05	3.13E+05	1.15E+06	1.07E+06	5.49E+05	6.27E+05
	6	1.12E+05	1.07E+05	5.18E+04	5.88E+04	5.59E+05	5.33E+05	2.59E+05	2.94E+05	1.12E+06	1.07E+06	5.18E+05	5.88E+05
	8	1.09E+05	1.05E+05	4.93E+04	5.59E+04	5.43E+05	5.26E+05	2.47E+05	2.80E+05	1.09E+06	1.05E+06	4.93E+05	5.59E+05
	10	1.05E+05	1.03E+05	4.73E+04	5.36E+04	5.26E+05	5.15E+05	2.36E+05	2.88E+05	1.05E+06	1.03E+06	4.73E+05	5.38E+05
	12	1.02E+05	1.100E+05	4.54E+04	5.16E+04	5.08E+05	5.10E+05	2.27E+05	2.58E+05	1.02E+06	1.00E+06	4.54E+05	5.16E+05
	14	9.78E+04	9.69E+04	4.36E+04	4.97E+04	4.89E+05	4.84E+05	2.18E+05	2.49E+05	9.78E+05	9.69E+05	4.36E+05	4.97E+05
	16	9.39E+04	9.33E+04	4.19E+04	4.79E+04	4.70E+05	4.67E+05	2.10E+05	2.40E+05	9.39E+05	9.33E+05	4.19E+05	4.79E+05
	18	9.00E+04	8.96E+04	4.03E+04	4.61E+04	4.50E+05	4.48E+05	2.01E+05	2.31E+05	9.00E+05	8.96E+05	4.03E+05	4.61E+05
	20	8.61E+04	8.58E+04	3.87E+04	4.44E+04	4.30E+05	4.29E+05	1.93E+05	2.22E+05	8.61E+05	8.58E+05	3.87E+05	4.44E+05
1		7.83E+04	7.81E+04	3.56E+04	4.09E+04	3.92E+05	3.91E+05	1.78E+05	2.04E+05	7.83E+05	7.81E+05	3.56E+05	4.09E+05
2		4.28E+04	4.11E+04	2.20E+04	2.44E+04	2.14E+05	2.01E+05	1.10E+05	1.22E+05	4.28E+05	4.11E+05	2.20E+05	2.44E+05
3		2.57E+04	2.27E+04	1.55E+04	1.61E+04	1.29E+05	1.14E+05	7.74E+04	8.05E+04	2.57E+05	2.27E+05	1.55E+05	1.61E+05
4		1.86E+04	1.50E+04	1.27E+04	1.25E+04	9.28E+04	7.48E+04	6.35E+04	6.27E+04	1.86E+05	1.50E+05	1.27E+05	1.25E+05
5		1.56E+04	1.18E+04	1.15E+04	1.10E+04	7.81E+04	5.90E+04	5.74E+04	5.51E+04	1.56E+05	1.18E+05	1.15E+05	1.10E+05
6		1.43E+04	1.05E+04	1.09E+04	1.03E+04	7.15E+04	5.23E+04	5.44E+04	5.15E+04	1.43E+05	1.05E+05	1.09E+05	1.03E+05
7		1.38E+04	9.80E+03	1.05E+04	9.89E+03	6.82E+04	4.90E+04	5.26E+04	4.94E+04	1.36E+05	9.80E+04	1.05E+05	9.89E+04
8		1.32E+04	9.42E+03	1.03E+04	9.61E+03	6.61E+04	4.71E+04	5.13E+04	4.80E+04	1.32E+05	9.42E+04	1.03E+05	9.61E+04
9		1.29E+04	9.15E+03	1.00E+04	9.39E+03	6.45E+04	4.58E+04	5.02E+04	4.69E+04	1.29E+05	9.15E+04	1.00E+05	9.39E+04
10		1.26E+04	8.93E+03	9.84E+03	9.19E+03	6.31E+04	4.47E+04	4.92E+04	4.56E+04	1.26E+05	8.93E+04	9.84E+04	9.19E+04
15		1.17E+04	8.20E+03	9.11E+03	8.48E+03	5.83E+04	4.10E+04	4.56E+04	4.24E+04	1.17E+05	8.20E+04	9.11E+04	8.48E+04

Time Since Intake		Ludlum 12S Survey Meter (Distance from Surface of 50th Percentile Adult Female: 30 cm)											
		Net Count Rate (cpm) for 50 mSv ED				Net Count Rate (cpm) for 250 mSv ED				Net Count Rate (cpm) for 500 mSv ED			
Time (days)	Time (hours)	AP Chest	AP Abdomen	PA Chest	PA Abdomen	AP Chest	AP Abdomen	PA Chest	PA >Abdomen	AP Chest	AP Abdomen	PA Chest	PA Abdomen
20		1.07E+04	7.47E+03	8.38E+03	7.78E+03	5.35E+04	3.73E+04	4.19E+04	3.89E+04	1.07E+05	7.47E+04	8.33E+04	7.78E+04
25		1.01E+04	7.02E+03	7.89E+03	7.32E+03	5.03E+04	3.51E+04	3.94E+04	3.66E+04	1.01E+05	7.02E+04	7.89E+04	7.32E+04
30		9.43E+03	6.58E+03	7.39E+03	6.88E+03	4.72E+04	3.29E+04	3.70E+04	3.43E+04	9.43E+04	6.58E+04	7.39E+04	6.88E+04

Table 6

Representative table from Handbook F on the use of the Ludlum 12S survey meter for radiological triage screening of the adult female at distances of 100 and 200 cm. Exposure scenario 6: acute inhalation of ^{60}Co aerosol at μm AMAD and solubility class Type M.

Time Since Intake		Ludlum 12S Surver Meter (Distance from Surface of 50th Percentile Adult Female: 100 cm)											
		Net Count Rate (com) for 50 mSv ED				Net Count Rate (com) for 250 mSv ED				Net Count Rate (com) for 500 mSv ED			
Time (days)	Time (hours)	AP Chest	AP Abdomen	PA Chest	PA Abdomen	PA Chest	AP Abdomen	PA Chest	PA Abdomen	AP Chest	AP Abdomen	PA Chest	PA Abdomen
	0.5	1.99E+04	1.81E+04	1.34E+04	1.26E+04	9.95E+04	9.03E+04	6.70E+04	6.32E+04	1.99E+05	1.81E+05	1.34E+05	1.26E+05
	1	2.02E+04	1.86E+04	1.36E+04	1.30E+04	1.01E+05	9.28E+04	6.80E+04	6.48E+04	2.02E+05	1.86E+05	1.36E+05	1.30E+05
	2	1.98E+04	1.85E+04	1.32E+04	1.26E+04	9.91E+04	9.26E+04	6.62E+04	6.28E+04	1.98E+05	1.85E+05	1.32E+05	1.26E+05
	4	1.94E+04	1.83E+04	1.23E+04	1.16E+04	9.71E+04	9.13E+04	6.13E+04	5.82E+04	1.94E+05	1.83E+05	1.23E+05	1.16E+05
	6	1.90E+04	1.78E+04	1.14E+04	1.09E+04	9.52E+04	8.92E+04	5.72E+04	5.47E+04	1.90E+05	1.78E+05	1.14E+05	1.09E+05
	8	1.86E+04	1.73E+04	1.08E+04	1.04E+04	9.30E+04	8.66E+04	5.40E+04	5.20E+04	1.86E+05	1.73E+05	1.08E+05	1.04E+05
	10	1.81E+04	1.67E+04	1.03E+04	9.94E+03	9.03E+04	8.35E+04	5.13E+04	4.97E+04	1.81E+05	1.67E+05	1.03E+05	9.94E+04
	12	1.75E+04	1.60E+04	9.78E+03	9.53E+03	8.74E+04	8.02E+04	4.89E+04	4.77E+04	1.75E+05	1.60E+05	9.78E+04	9.53E+04
	14	1.68E+04	1.54E+04	9.34E+03	9.15E+03	8.42E+04	7.68E+04	4.67E+04	4.57E+04	1.68E+05	1.54E+05	9.93E+04	9.15E+04
	16	1.62E+04	1.47E+04	8.93E+03	8.78E+03	8.09E+04	7.34E+04	4.47E+04	4.39E+04	1.62E+05	1.47E+05	9.34E+04	8.78E+04
	18	1.55E+04	1.40E+04	8.54E+03	8.43E+03	7.75E+04	7.00E+04	4.27E+04	4.21E+04	1.55E+05	1.40E+05	8.93E+04	8.43E+04
	20	1.48E+04	1.33E+04	8.16E+03	8.08E+03	7.42E+04	6.66E+04	4.08E+04	4.04E+04	1.48E+05	1.33E+05	8.16E+04	8.08E+04
1		1.35E+04	1.20E+04	7.44E+03	7.41E+03	6.75E+04	6.01E+04	3.72E+04	3.71E+04	1.35E+05	1.20E+05	7.44E+04	7.41E+04
2		7.34E+03	6.36E+03	4.38E+03	4.46E+03	3.67E+04	3.18E+04	2.19E+04	2.23E+04	7.34E+04	6.36E+04	4.38E+04	4.46E+04
3		4.35E+03	3.75E+03	2.96E+03	3.05E+03	2.18E+04	1.88E+04	1.48E+04	1.53E+04	4.35E+04	3.75E+04	2.96E+04	3.05E+04
4		3.10E+03	2.67E+03	2.35E+03	2.45E+03	1.55E+04	1.33E+04	1.18E+04	1.23E+04	3.10E+04	2.67E+04	2.35E+04	2.45E+04
5		2.58E+03	2.22E+03	2.09E+03	2.19E+03	1.29E+04	1.11E+04	1.05E+04	1.09E+04	2.58E+04	2.22E+04	2.03E+04	2.19E+04
6		2.35E+03	2.03E+03	1.97E+03	2.06E+03	1.17E+04	1.01E+04	9.85E+03	1.03E+04	2.35E+04	2.03E+04	1.97E+04	2.06E+04
7		2.23E+03	1.93E+03	1.90E+03	1.99E+03	1.11E+04	9.64E+03	9.48E+03	9.94E+03	2.23E+04	1.93E+04	1.90E+04	1.99E+04
8		2.15E+03	1.86E+03	1.84E+03	1.94E+03	1.08E+04	9.32E+03	9.22E+03	9.68E+03	2.15E+04	1.86E+04	1.84E+04	1.94E+04
9		2.10E+03	1.82E+03	1.80E+03	1.89E+03	1.05E+04	9.08E+03	9.01E+03	9.46E+03	2.10E+04	1.82E+04	1.80E+04	1.89E+04
10		2.05E+03	1.78E+03	1.76E+03	1.85E+03	1.03E+04	8.88E+03	8.82E+03	9.27E+03	2.05E+04	1.78E+04	1.76E+04	1.85E+04
15		1.87E+03	1.62E+03	1.61E+03	1.70E+03	9.34E+03	8.09E+03	8.05E+03	8.48E+03	1.87E+04	1.62E+04	1.61E+04	1.70E+04
20		1.73E+03	1.50E+03	1.49E+03	1.57E+03	8.64E+03	7.48E+03	7.46E+03	7.86E+03	1.73E+04	1.50E+04	1.49E+04	1.57E+04
25		1.62E+03	1.41E+03	1.40E+03	1.48E+03	8.12E+03	7.04E+03	7.02E+03	7.40E+03	1.62E+04	1.41E+04	1.40E+04	1.48E+04

Time Since Intake		Ludlum 12S Surver Meter (Distance from Surface of 50th Percentile Adult Female: 100 cm)											
		Net Count Rate (com) for 50 mSv ED				Net Count Rate (com) for 250 mSv ED				Net Count Rate (com) for 500 mSv ED			
Time (days)	Time (hours)	AP Chest	AP Abdomen	PA Chest	PA Abdomen	PA Chest	AP Abdomen	PA Chest	PA Abdomen	AP Chest	AP Abdomen	PA Chest	PA Abdomen
30		1.52E+03	1.32E+03	1.32E+03	1.39E+03	7.81E+03	6.59E+03	6.58E+03	6.94E+03	1.52E+04	1.32E+04	1.32E+04	1.39E+04

Time Since intake		Ludlum 125 survey meter (Distance from Surface of 50th percentile Adult Female: 200 cm)											
		Net Count Rate (cpm) for 50 msv ED				Net Count Rate (cpm) for 250 msv ED				Net Count Rate (cpm) for 500 msv ED			
Time (days)	Time (hours)	AP Chest	AP Abdomen	PA Cheat	PA Abdomen	AP Chest	AP Abdomen	PA Cheat	PA Abdomen	AP Cheat	AP Abdomen	PA Chess	PA Abdomen
	0.5	5.31E+03	5.31E+03	4.02E+03	4.02E+03	2.65E+04	2.65E+04	2.01E+04	2.01E+04	5.31E+04	5.31E+04	4.02E+04	4.02E+04
	1	5.29E+03	5.29E+03	3.96E+03	3.96E+03	2.64E+01	2.64E+04	1.98E+04	1.98E+04	5.28E+04	5.29E+04	3.96+04	3.96E+04
	2	5.24E+03	5.24E+03	3.80E+03	3.80E+03	2.62E+04	2.62E+04	1.90E+04	1.90E+04	5.24E+04	5.24E+04	3.80E+04	3.80E+04
	4	5.16E+03	5.16E+03	3.53E+03	3.53E+03	2.58E+04	7.58E+04	1.77E+04	1.77E+04	5.16E+04	5.16E+04	3.63E+04	3.53E+04
	6	5.05E+03	5.05E+03	3.34E+03	3.34E+03	2.53E+04	2.53E+04	1.67E+04	1.67E+04	5.05E+04	5.05E+04	3.34E+04	3.34E+04
	8	4.90E+03	4.90E+03	3.18E+03	3.18E+03	2.45E+04	2.45E+04	1.59E+04	1.59E+04	4.90E+04	4.90E+04	3.18E+04	3.18E+04
	10	4.74E+03	4.74E+03	3.04E+03	3.04E+03	2.37E+04	2.37E+04	1.52E+04	1.52E+04	4.74E+04	4.74E+04	3.04E+04	3.04E+04
	12	4.56E+03	4.56E+03	2.92E+03	2.92E+03	2.28E+04	2.28E+04	1.46E+04	1.46E+04	4.56E+04	4.56E+04	2.92E+04	2.92E+04
	14	4.37E+03	4.37E+03	2.80E+03	2.80E+03	2.19E+04	2.19E+04	1.40E+04	1.40E+04	4.37E+04	4.37E+04	2.80E+04	2.80E+04
	16	4.18E+03	4.18E+03	2.89E+03	2.69E+03	2.09E+04	2.09E+04	1.34E+04	1.34E+04	4.18E+04	4.18RE+04	2.69E+04	2.69E+04
	18	3.99E+03	3.99E+03	2.58E+03	2.58E+03	2.00E+04	2.00E+04	1.29E+04	1.29E+04	3.99E+04	3.99E+04	2.58E+04	2.58E+04
	20	3.81E+03	3.81E+03	2.47E+03	2.47E+03	1.90E+04	1.90E+04	1.23E+04	1.23E+04	3.81E+04	3.81E+04	2.47E+04	2.47E+04
1		3.45E+03	3.45E+03	2.26E+03	2.26E+03	1.72E+04	1.72E+04	1.13E+04	1.13E+04	3.45E+04	3.45E+04	2.28E+04	2.26E+04
2		1.88E+03	1.88E+03	1.32E+03	1.32E+03	9.41E+03	9.41E+03	6.60E+03	6.60E+03	1.88E+04	1.88E+04	1.32E+04	1.32E+04
3		1.16E+03	1.16E+03	8.72E+02	8.72E+02	5.79E+03	5.79E+03	4.36E+03	4.36E+03	1.16E+04	1.16E+04	8.72E+03	8.72E+03
4		8.56E+02	8.56E+02	6.81E+02	6.81E+02	4.28E+03	4.28E+03	3.41E+03	3.41E+03	8.56E+03	8.56E+03	6.81E+03	6.81E+03
5		7.30E+02	7.30E+02	6.00E+02	6.00E+02	3.65E+03	3.65E+03	3.00E+03	3.00E+03	7.30E+03	7.30E+03	6.00E+03	6.00E+03
6		6.73E+02	6.73E+02	5.61E+02	5.61E+02	3.371E+03	3.37E+03	2.81E+03	2.81E+03	6.73E+03	6.73E+03	5.61E+03	5.61E+03
7		6.43E+02	6.43E+02	5.40E+02	5.40E+02	3.22E+03	3.22E+03	2.70E+03	2.70E+03	6.43E+03	8.43E+03	5.40E+03	5.40E+03
8		6.24E+02	6.24E+02	5.24E+02	5.24E+02	3.12E+03	3.12E+03	2.62E+03	2.62E+03	6.24E+03	6.24E+03	5.24E+03	5.24E+03
9		6.O9E+02	6.09E+02	5.12E+02	5.12E+02	3.04E+03	3.04E+03	2.56E+03	2.56E+03	6.09E+03	6.09E+03	5.12E+03	5.12E+03
10		5.96E+02	5.96E+02	5.02E+02	5.02E+02	2.98E+03	2.98E+03	2.51E+03	2.51E+03	5.96E+03	5.96E+03	5.02E+03	5.02E+03
15		5.44E+02	5.44E+02	4.5SE+02	4.58E+02	2.72E+03	2.72E+03	2.29E+03	2.29E+03	5.44E+03	5.44E+03	4.58E+03	4.58E+03

Time Since intake		Ludlum 125 survey meter (Distance from Surface of 50th percentile Adult Female: 200 cm)											
		Net Count Rate (cpm) for 50 msv ED				Net Count Rate (cpm) for 250 msv ED				Net Count Rate (cpm) for 500 msv ED			
Time (days)	Time (hours)	AP Chest	AP Abdomen	PA Cheat	PA Abdomen	AP Chest	AP Abdomen	PA Cheat	PA Abdomen	AP Cheat	AP Abdomen	PA Chess	PA Abdomen
20		5.04E+02	5.04E+02	4.25E+02	4.26E+02	2.52E+03	2.52E+03	2.12E+03	2.12E+03	5.04E+03	5.04E+03	4.25E+03	4.25E+03
25		4.74E+02	4.74E+02	4.00E+02	4.00E+02	2.37E+03	2.37E+03	2.00E+03	2.00E+03	4.74E+03	4.74E+03	4.00E+03	4.00E+03
30		4.44E+02	4.44E+02	3.75E+02	3.75E+02	2.22E+03	2.22E+03	1.87E+03	1.87E+03	4.44E+03	4.44E+03	3.75E+03	3.75E+03

Table 7

Recommendations for medical response following radiological triage screening by radionuclide and estimated range of effective dose based on survey meter count rate measurements.

	Ranges of Effective Dose and Their Corresponding Recommended Medical Response			
	Effective Dose	Effective Dose	Effective Dose	Effective Dose
	< 50 mSv	*50–250 mSv*	*250–500 mSv*	*>500 mSv*
Radionuclide	***Triage Condition I***	***Triage Condition II***	***Triage Condition III***	***Triage Condition IV***
Am-241	**K**	**K, M**	**A, B, C, D, E, F, L, M**	**A, B, C, D, E, F, J, L, M**
Co-60	**K**	**K, M**	**A, B, C, D, E, F, L, M**	**A, B, C, D, E, F, J, L, M**
Cs-137	**K**	**K, M**	**A, B, C, D, E, G, L, M**	**A, B, C, D, E, G, J, L, M**
I–131	**K**	**K, M**	**H, L, M**	**H, L, M**
Ir-192	**K**	**K, M**	**A, B, C, D, E, I, L, M**	**A, B, C, D, E, I, J, L, M**

Recommendations based on availability of resources:

A If medical evaluation is within 30–60 minutes of inhalation, perform nasal swabs (see NCRP Report No. 161)

B If medical evaluation is within 24 hours of ingestion, provide cathartics

C Obtain baseline Complete Blood Count (CBC), Serum Electrolytes, and Chemistry Panel

D Collect 24-hour urine and stool samples for bioassay analysis

E Obtain serial CBCs every 8 to 12 hours for 3 days, and then daily for an additional 4 days to rule out Acute Radiation Syndrome.

F Prescribe DTPA per FDA guidelines (see FDA website or NCRP Report No. 161). DTPA is FDA approved only for chelation of americium, curium, and plutonium. Other uses of DTPA are off-label. If DTPA will not be available for several hours, consider initiating EDTA treatment per FDA guidelines. EDTA is FDA approved only for lead poisoning. Other uses of EDTA are off-label. Change to DTPA when available.

G Prescribe Prussian Blue (Ferric Ferrocyanate, Radiogardase®) per FDA guidelines (see FDA website or NCRP Report No. 161). Prussian Blue is FDA-approved only for cesium and thallium intakes. Other uses are off-label.

H Prescribe potassium iodide (KI) per FDA guidelines. KI is FDA-approved only for treatment of radioactive iodine (RAI) intake. Criteria for treatment and dosing is dependent on subject age and pregnancy and lactation status.

I There is limited clinical experience with the use of DTPA or EDTA for internal contamination with iridium. Recommend to consider using DTPA off-label and follow FDA drug guidance. If DTPA is not available, consider using EDTA off-label.

J At the physician's discretion, consider performing lung lavage for inhalational injury with effective dose > 2000 mSv based on risk/benefit

K Follow-up with primary care physician for routine cancer screening.

L Follow-up with primary care physician for high-risk cancer screening.

M Confirm triage condition (dose range) via (1) urine bioassay, (2) whole-body counting, or (3) gamma-camera imaging (see http://www.bt.cdc.gov/radiation/ clinicians/evaluation)

Table 8

Time-dependent detector count rate thresholds for a 250 mSv effective dose for different ^{192}Ir inhalation and ingestion exposure scenarios relative to corresponding values for a reference inhalation exposure for a 1-μm ANTAD Type M aerosol. All values are taken for the Ludlum 12S survey meter screening an adult female subject in the AP (chest or abdomen) position at 200 cm.

	1 μm AMAD			5 μm AMAD			
	Type F	Type M	Type S	Type F	Type M	Type S	Ingestion
Time (days)	Ratio	Ref	Ratio	Ratio	Ratio	Ratio	Ratio
0.01	2.72	1.00	0.79	3.79	2.05	1.71	7.78
0.04	2.67	1.00	0.79	3.71	2.06	1.73	7.69
0.06	2.66	1.00	0.79	3.69	2.05	1.72	7.77
0.10	2.65	1.00	0.79	3.67	2.05	1.72	7.90
0.40	2.62	1.00	0.79	3.54	2.00	1.69	8.59
0.60	2.62	1.00	0.79	3.48	1.97	1.65	8.75
1.00	2.69	1.00	0.79	3.45	1.87	1.57	8.53
2.00	3.07	1.00	0.78	3.55	1.55	1.27	6.36
4 00	3.79	1.00	0.76	3.87	1.02	0.75	1.81
6.00	3.96	1.00	0.75	3.94	0.86	0.61	0.46
8 00	3.96	1.00	0.75	3.92	0.83	0.58	0.25
1 0.00	3.94	1.00	0.76	3.90	0.83	0.58	0.21
20.00	3.91	1.00	0.76	3.86	0.82	0.58	0.21
30.00	3.95	1.00	0.77	3.91	0.82	0.58	0.21

Table 9

Ratios of the count rate thresholds (250 mSv effective dose) for the adult female to corresponding values for the adult male as a function of time post-intake and detector screening distance. The exposure is an I ingestion exposure, and the screening is performed in the AP chest position using a Ludlum 12S survey meter.

	Screening distance - AP chest			
Time (days)	6 cm ratio F/M	30 cm ratio F/M	100 cm ratio F/M	200 cm ratio F/M
0.01	1.03	1.12	1.10	1.05
0.04	1.35	1.24	1.16	1.09
0.06	1.57	1.32	1.20	1.11
0.10	1.74	1.38	1.22	1.13
0.40	1.57	1.26	1.16	1.08
0.60	139	1.17	1.11	1.05
1.00	1.16	1.06	1.04	1.01
2.00	1.00	1.00	1.00	0.98
4.00	0.99	1.00	1.00	0.98
8.00	0.99	1.00	1.00	0.98
10.00	0.99	1.00	1.00	0.98
20.00	0.98	1.00	1.01	0.98
30.00	0.98	1.01	1.01	0.98